

Article

# U-Pb Ages and Hf Isotopes of Detrital Zircon Grains from the Mesoproterozoic Chuanlinggou Formation in North China Craton: Implications for the Geochronology of Sedimentary Iron Deposits and Crustal Evolution

**Chao Duan** <sup>1,\*</sup>, **Yanhe Li** <sup>1,\*</sup>, **Yun Yang** <sup>2</sup>, **Yongsheng Liang** <sup>2</sup>, **Minghui Wei** <sup>2</sup> and **Kejun Hou** <sup>1</sup><sup>1</sup> Ministry of Natural Resources Key Laboratory of Metallogeny and Mineral Assessment, Institute of Mineral Resources, Chinese Academy of Geological Sciences, Beijing 100037, China; kejunhou@126.com<sup>2</sup> No. 3 Geological Brigade, Hebei Geological and Mineral Exploration Bureau, Zhangjiakou 075000, China; yangyun5905905@163.com (Y.Y.); liangyongshengcool@163.com (Y.L.); wmh.137@163.com (M.W.)

\* Correspondence: duanchao@cags.ac.cn (C.D.); lyh@cei.gov.cn (Y.L.)

Received: 6 September 2018; Accepted: 21 November 2018; Published: 26 November 2018



**Abstract:** The Chuanlinggou Formation is the lower formation of the Changchengian System, and hosts sedimentary iron deposits (marine oolitic ironstones) of the North China Craton (NCC). To determine the age of the iron deposits, and provide insight into the crustal growth of the craton, laser ablation multiple collector inductively coupled plasma mass spectrometry (LA-MC-ICP-MS)U-Pb and in situ Hf isotope analysis were performed on detrital zircon grains. Samples were taken from the roof sand-shale of the sedimentary iron deposits at Jiangjiazhai and Pangjiapu. Overall, 186 detrital zircon grain U-Pb ages yield three major age populations, with weighted average ages of 2450 Ma, 1848 Ma, and 1765 Ma, respectively. Four younger ages from magmatic zircon grains were obtained, ranging from 1694 to 1657 Ma. Combined with observations from published studies, the results define the lower limit for the age of the Chuanlinggou Formation, and constrain the age of the sedimentary iron deposits (marine oolitic ironstone) close to 1650 Ma. The peak ages of 1848 Ma and 2450 Ma define the major collisional events of the NCC. The age of 1765 Ma can be linked to the age range of the widespread mafic dyke swarms that represent the rifting of the NCC within the Columbia supercontinent. Detrital zircon grains from the Chuanlinggou Formation form two obvious groups, with different  $\epsilon$ Hf ( $t$ ) values ranging from  $-1$  to  $-8$  and from  $+1$  to  $+8$ , which correspond to the U-Pb age ranges of 1.7–1.9 Ga and 2.3–2.6 Ga, respectively. They have a similar two-stage Hf model age peak at 2.65–2.85 Ga, suggesting that the source rocks for each of these events were derived from the recycling of ancient crust. The source rocks of the older group of zircon grains might be derived from juvenile crust with a short reworking period. The critical crust–mantle differentiation event might happen during the period of 2.65–2.85 Ga, marking the most significant stage of the crustal growth in the NCC.

**Keywords:** Chuanlinggou Formation; detrital zircon U-Pb age; Hf isotope; sedimentary iron deposit; North China Craton

## 1. Introduction

The North China Craton (NCC) covers an area of about 1.5 million km<sup>2</sup> and is one of the oldest cratons, with age components as old as ~3.8 Ga [1–3]. The craton is bounded by the early Palaeozoic Qilianshan Orogen and late Palaeozoic Central Asian Orogenic Belt to the west and north, and the Mesozoic Qinling–Dabie and Su–Lu ultrahigh-pressure metamorphic belts to the south and east,

respectively (Figure 1). From the Archean, the craton experienced a geological history containing many recorded tectonic and metamorphic events [2,4–12]. Three main models for the formation of the NCC have been proposed using stratigraphic, structural, metamorphic, geochemical, and geochronological studies. (1) The NCC was originally divided into several micro-blocks (Jiaoliao, Qianhuai, Fuping, Jining, Xuchang, and Alashan), which formed the final craton during the late Neoarchean (~2.5 Ga) [3,6,13–17]; (2) Zhao et al. (2001, 2005, 2012) [1,2,7] suggested a model for the evolution of the NCC, which divided the NCC into three parts: the Western Block, Eastern Block, and Trans-North China Orogeny (TNCO) (Figure 1). Prior to the collision of the Western and Eastern blocks along the TNCO at ~1.85 Ga, the Western Block was formed by the amalgamation of the Ordos Block in the south and the Yinshan Block in the north, along the east–west-trending Khondalite Belt, and the Eastern Block underwent a Paleoproterozoic rifting event along its eastern continental margin in the period 2.2–1.9 Ga, forming the Jiao-Liao-Ji Belt [18–24]; (3) Another model suggests that the Eastern and Western blocks were amalgamated at ca. 2.5 Ga, and that at ca. 1.85 Ga the Central Orogenic Belt experienced a metamorphic reworking/overprinting by the collision of the northern margin of the NCC with another continental block in the Columbia (Nuna) Supercontinent [25–28].

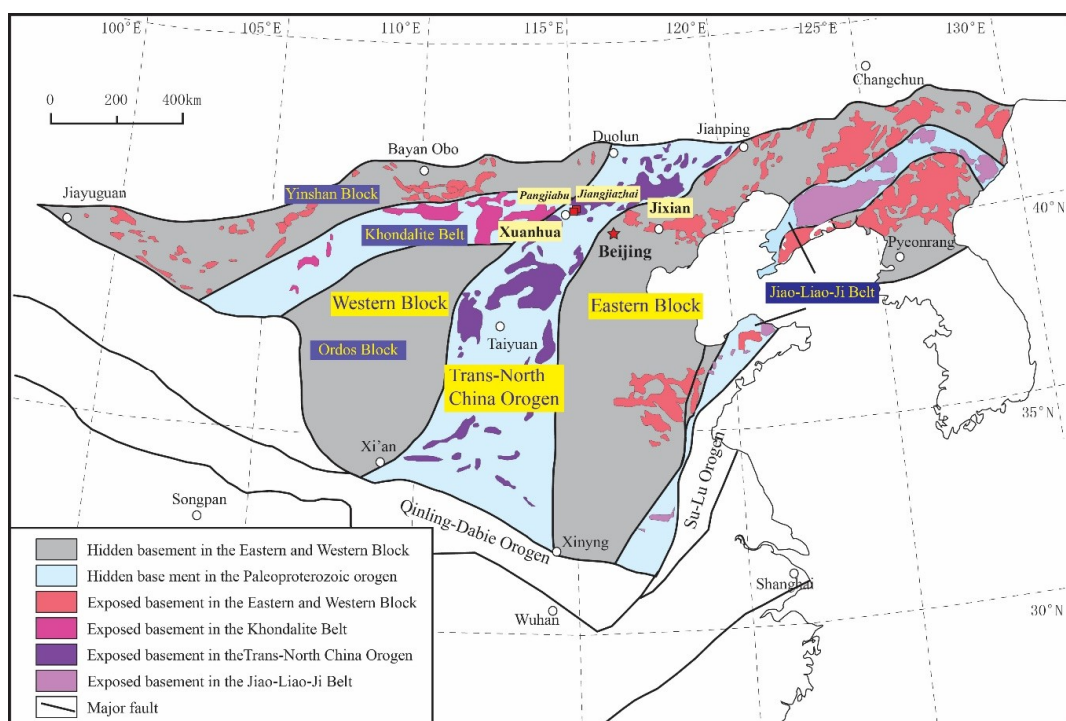


**Figure 1.** Tectonic subdivision of the North China Craton (modified after Zhao et al., 2012 [7]).  
Pangjiabu and Jiangjiazhai are the sampling locations.

The North China Craton is rich in mineral resources; the Precambrian is one of the critical mineralization periods, which is marked by the appearances of large iron, rare earth elements, lead–zinc, and magnetite deposits [29,30]. Precambrian iron deposits are the most important mineral resource in the North China Craton, of which the banded iron formation (BIF) type is predominant, accounting for ~80% of metamorphosed sedimentary iron ores in China, with a peak formation age of 2.5–2.6 Ga [31–37]. Marine oolitic ironstone is another type of sedimentary hosted iron ore in the NCC, referred to as the Xuanlong type deposit in the Chinese literatures. The oolitic iron deposit is a distinctive subset of iron deposits, characterized by spherical grains composed of concentric layers containing hematite and goethite. Different to BIF, most deposits of this type have a biogenic origin. As a result of its special genesis environment, oolitic iron ores also provide much significant information about the evolution of palaeogeographic facies and marine chemical conditions [38–40].

Oolitic iron ores (ironstones) occur worldwide and were formed throughout the geological time from the Proterozoic Eon to the Cenozoic Era. In the NCC, it is considered to have occurred in the Mesoproterozoic, hosted in the Chuanlinggou Formation. However, the geochronology of the Chuanlinggou Formation with the oolitic iron deposit is still poorly understood.

In this study, we present U-Pb ages and Hf isotope data from detrital zircon grains from sand-shale samples collected from the roof of the sedimentary iron ores at Jiangjiazhai and Pangjiabu (Figure 1), in order to determine the chronology of the iron deposition, supplying a piece of the picture of the time frame of the distribution of oolitic iron deposits in the global context, and provide further information on the crustal growth and evolution of the NCC.

## 2. Geological Setting

### 2.1. Regional Geology

In the NCC, the marine oolitic ironstones are located in the Trans-North China Orogeny (TNCO), which was defined by Zhao et al. (2001, 2005) [1,2], with boundaries of the Xinyang–Kaifeng–Shijiazhaung–Jianping fault zone and the Huashan–Lishi–Datong–Duolun fault zone. During the late Archean to early Paleoproterozoic, the western margin of the Eastern Block faced a major ocean, and east-dipping subduction beneath the western margin of the Eastern Block led to the formation of magmatic arcs that were subsequently incorporated into the TNCO [7]. Continued subduction resulted in a major continental–continental collision, leading to extensive thrusting and high-pressure metamorphism. During the period 2.56–1.85 Ga, the Huai'an, Hengshan, Wutai, Fuping, Zanhua, Lvliang, Zhongtiao, Dengfeng, Taihua, and other metamorphic complexes formed in the TNCO [41,42], providing records of the tectonic activity. The available age data for metamorphism and deformation in the Trans-North China Orogen indicate that this collisional event occurred at about 1.85 Ga ago, resulting in the formation of the TNCO and final amalgamation of the North China Craton [7,43]. After 1.80 Ga, the NCC experienced extensional tectonism, marked by the development of large mafic and alkaline intrusions [9,16,44]. The North China Craton experienced large-scale sedimentation in the Mesoproterozoic, forming the Changchengian System and the Jixianian System. The Changchengian System (~3000 m thick) contains four units from its base to top; the Changzhougou Formation (~860 m thick), Chuanlinggou Formation (~890 m thick), Tuanshanzi Formation (~520 m thick) and Dahongyu Formation (~480 m thick) (Zhang et al., 2015 [45] and references therein).

### 2.2. Chuanlinggou Formation

The Chuanlinggou Formation is widely distributed in North China and can be divided into three depositional regions. The eastern area, including Jixian, Zunhua, Xinglong, and Kuancheng, is characterized by the development of thick black shale. The middle area is located in the northern part of Miyun–Huairou and comprises lacustrine dolomite and lagoon facies depositions. The western area is located in the Xuanhua–Zhangjiakou area, where the thickness of the formation is significantly thinner, and is characterized by the development of the sedimentary iron rocks. Xuanlong type iron deposits occurred in this typical area.

The type profile of the Chuanlinggou Formation is divided into three members [46] (Figure 2a). Member one contains yellowish brown sandy shale with yellow-green siltstone and iron-rich sandstone. Clay minerals are mainly illite. Sandstone, siltstone, and shale exhibit obvious rhythmic sedimentary characteristics, with horizontal bedding and microwave bedding, mud cracks, and ripple level structures. The maximum thickness of one single rhythm is 127 mm; member two is mainly composed of black and dark grey silty shale, locally intercalated with thin silty bars and dolomite, with horizontal bedding. The silty shale is the basic rhythmic layer and is less than 1 cm thick; and member three is composed of black silty shale and greyish white thin siltstone, with 2–3 layers of lightly colored microcrystalline carbonaceous dolomite at the top, with wavy and horizontal bedding. Some bedding planes show mud cracks and underwater sliding load curling structures.

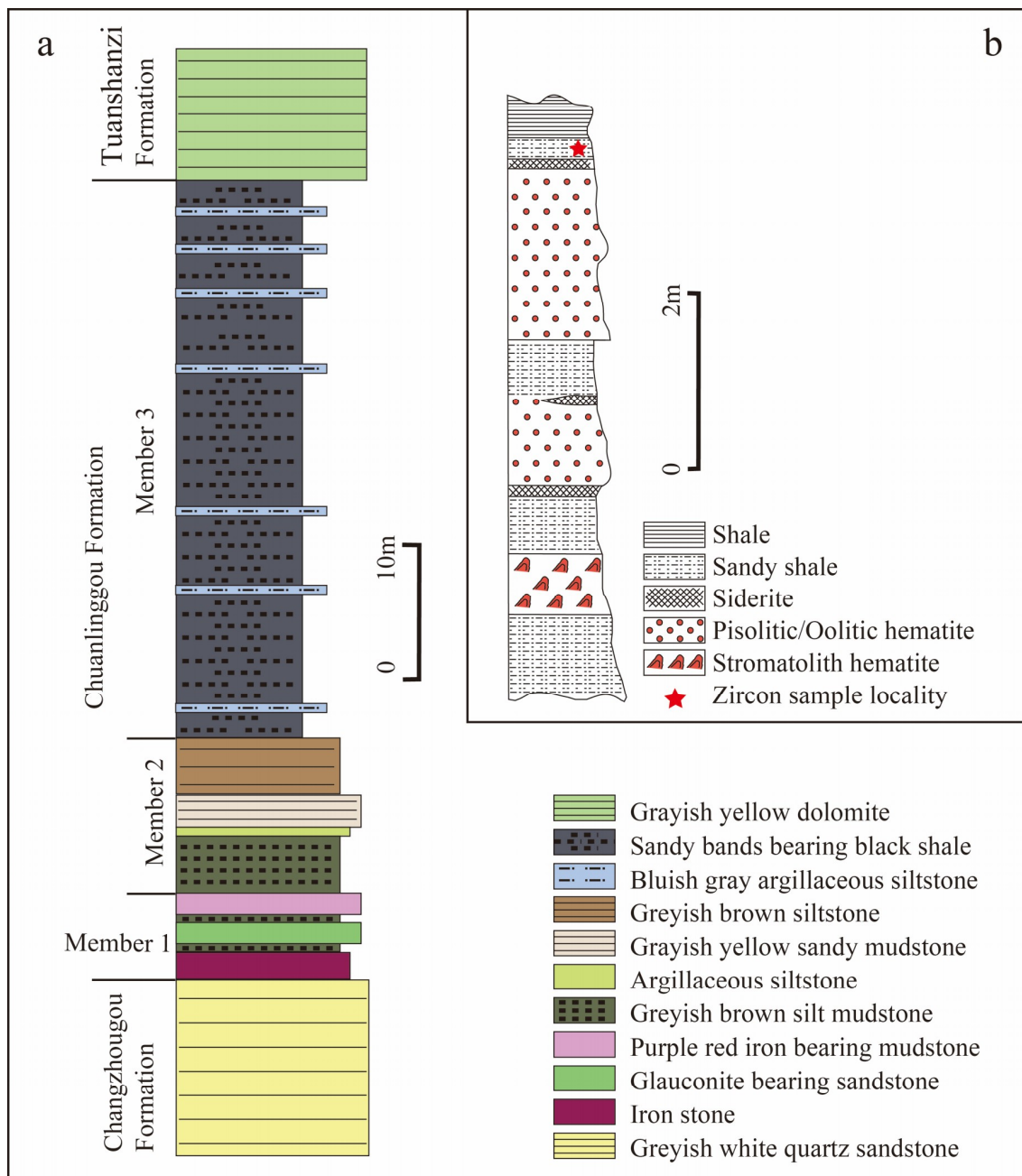


**Figure 2.** (a) Ironstone and related sedimentary successions in the Chuanlinggou Formation at the Xuanhua area (modified after Tang et al., 2015 [47]); (b) A representative iron ore-bearing sequence of the Chuanlinggou Formation (modified after Zhao, 1994 [48]).

The Chuanlinggou Formation contains three ironstone layers: the lower one is a stromatolite hematite, the middle is a pisolithic and oolitic hematite, and the upper part is an oolitic hematite (Figure 2b). Between the layers is a sandy shale unit. There are commonly siderite intercalations or thin lenses in the transitional parts of the shale and hematite layers. The stromatolite hematite is purplish red, usually upright without bending, developing a single tubular or bell-shaped aggregate structure. Quartz grains are deposited among the stromatolite hematite and are cemented by siderite or hematite. The pillar shaped stromatolite hematite has a diameter of 0.5–2 cm and a height of about 5 cm. The columnar bedding is fine and regular and has good symmetry. Oolitic hematite is dark red, of which 50–70% is oolitic. Ooids vary in size, have a particle size of 0.5–3 mm, and are mostly spherical or sub-spherical. Most of the terrigenous clastic material, primarily quartz, is deposited between

the oolitic grains. Most of the oolitic cores are single or clustered quartz grains, and sometimes they are also composed of iron debris and clay mineral mixtures, feldspar clasts and apatite fragments. The ooid shells have a transparent-translucent concentric ring structure and are composed mainly of hematite and siderite (Figure 3).

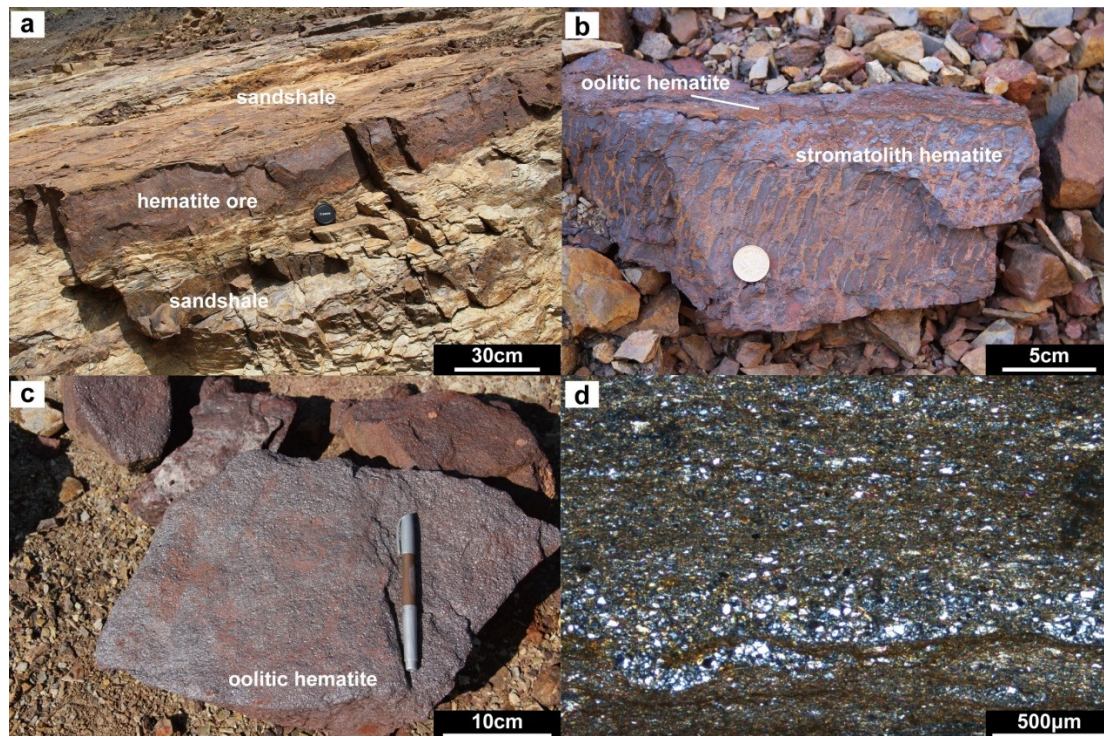


**Figure 3.** (a) Outcrop photo of the sandy shale; (b) photo of the stromatolith hematite ore with oolitic hematite appearing at the top; (c) photo of the oolitic hematite ore; (d) micrograph of the sandy shale.

The sedimentary iron deposits are mainly distributed in the Zhangjiakou area, the western part of the Yanshan, in the south of Huai'an–Chicheng and north of Huaxiaoying–Xiahuayuan–Xinglinbao. This covers an area of 3900 km<sup>2</sup>, with a length of 130 km oriented east-west and a width of 154 km running north-south. There are 23 Xuanlong type iron deposits in the belt, containing 304 million metric tons (Mt) of iron [49]. In this study, the samples analyzed were collected from the roof sand-shale (Figures 2 and 3) overlying the first hematite layer of the Chuanlinggou Formation in representative iron deposits at Jiangjiazhai (JJZ12-08, E 115°34'55" N 40°42'25") and Pangjiabu (PJB12-11, E 115°27'31" N 40°37'39") (Figure 1).

### 3. Analytical Methods

#### 3.1. Zircon LA-MC-ICP-MS U-Pb Dating

The samples were crushed and individual zircon grains were separated using conventional heavy liquid and magnetic techniques. Grains were handpicked under a binocular microscope, mounted in epoxy resin discs, and then polished. Zircon grains were examined under transmitted and reflected light, and then imaged by cathodoluminescence (CL) using a HITACHI S3000-N microprobe in the Institute of Mineral Resources, Geology Chinese Academy of Geological Sciences. The zircon grains, which were euhedral or subhedral, with a striped cathodoluminescence pattern and oscillatory zoning rims, were selected for U-Pb and Hf isotope dating.

U-Pb dating analyses were conducted by laser ablation multiple collector inductively coupled plasma mass spectrometry (LA-MC-ICP-MS) at the Institute of Mineral Resources, Chinese Academy of Geological Sciences, Beijing. Detailed operating conditions for the laser ablation system and the

MC-ICP-MS instrument and data reduction are the same as described by Hou et al. (2009) [50] and Liu et al. (2010) [51]. Laser sampling was performed using a New Wave UP 213 laser ablation system, with a beam diameter of 25  $\mu\text{m}$ . A Thermo Finnigan Neptune MC-ICP-MS instrument was used to acquire ion-signal intensities. The array of four multi-ion-counters and three Faraday cups allows for the simultaneous detection of  $^{202}\text{Hg}$  (on IC5),  $^{204}\text{Hg}$ ,  $^{204}\text{Pb}$  (on IC4),  $^{206}\text{Pb}$  (on IC3),  $^{207}\text{Pb}$  (on IC2),  $^{208}\text{Pb}$  (on L4),  $^{232}\text{Th}$  (on H2), and  $^{238}\text{U}$  (on H4) ion signals. Helium was used as a carrier gas. Argon was used as the make-up gas and mixed with the carrier gas via a T-connector before entering the ICP. Each analysis incorporated a background acquisition of approximately 20–30 s (gas blank) followed by 30 s of data acquisition from the sample. Off-line raw data selection and the integration of background and analyzed signals, as well as time-drift correction and quantitative calibration for U-Pb dating, were performed by ICPMSDataCal program [51]. Zircon GJ-1 was used as a reference material for U-Pb normalization, and was analyzed twice every 5–10 analyses. Time-dependent drifts of U-Th-Pb isotopic ratios were corrected using a linear interpolation (with time) for every 5–10 analyses according to the variations of GJ-1 (i.e., 2 GJ-1 zircon grains + 5–10 samples + 2 GJ-1 zircon grains) [51]. The preferred U-Th-Pb isotopic ratios used for GJ-1 are from Jackson et al. (2004) [52]. Uncertainty of preferred values for the external standard GJ-1 was propagated to the ultimate results of the samples. In all analyzed zircon grains, the common Pb correction has not been made due to the low signal of common  $^{204}\text{Pb}$  and high  $^{206}\text{Pb}/^{204}\text{Pb}$ . U, Th, and Pb concentrations were calibrated by zircon GJ-1 (with U:315 ppm and Th: 9.33 ppm; Liu et al., 2010 [51]). Concordia diagrams and weighted mean calculations were made using Isoplot 3.0 [53]. The reference zircon Plešovice was treated as an unknown and yielded the weighted mean  $^{206}\text{Pb}/^{238}\text{U}$  age of  $336.6 \pm 2.5$  Ma ( $2\sigma, n = 20$ ), which is in good agreement with the recommended  $^{206}\text{Pb}/^{238}\text{U}$  age of  $337.13 \pm 0.37$  Ma ( $2\sigma$ ) [54].

### 3.2. *In Situ* Zircon Lu-Hf Isotope Analyses

The zircon Hf analyses of two samples were performed on the same grains as used for U-Pb dating. Zircon Hf isotope analysis was carried out *in situ* using a New Wave UP 213 laser-ablation microprobe attached to a Neptune multi-collector ICP-MS at the Key Laboratory of Metallogeny and Mineral Assessment, Institute of Mineral Resources, Chinese Academy of Geological Sciences, Beijing. The same positions of zircon grains were used for the present analyses, with a beam diameter of 55  $\mu\text{m}$ . Helium was used as the carrier gas to transport the ablated sample from the laser-ablation cell to the ICP-MS torch, via a mixing chamber where it was mixed with argon. To correct the isobaric interferences of  $^{176}\text{Lu}$  and  $^{176}\text{Yb}$  on  $^{176}\text{Hf}$ , the  $^{176}\text{Lu}/^{175}\text{Lu}$  and  $^{176}\text{Yb}/^{173}\text{Yb}$  values were determined (0.02658 and 0.796218, respectively) [55]. For instrumental mass bias correction, Yb and Hf isotope ratios were normalized to 1.35274 for  $^{172}\text{Yb}/^{173}\text{Yb}$  [55] and to 0.7325 for  $^{179}\text{Hf}/^{177}\text{Hf}$  using an exponential law. The mass bias behavior of Lu was assumed to follow that of Yb. The mass bias correction protocols details are described in Wu et al. (2006) [56] and Hou et al. (2007) [57]. Zircon GJ-1 was used as the reference standards during our routine analyses, with a weighted mean  $^{176}\text{Hf}/^{177}\text{Hf}$  value of  $0.282017 \pm 0.000021$  ( $2\sigma, n = 13$ ). This is not distinguishable from the weighted mean  $^{176}\text{Hf}/^{177}\text{Hf}$  value of  $0.282000 \pm 0.000005$  ( $2\sigma$ ) using a solution analysis method by Morel et al. (2008) [58]. Also, a Temora zircon standard was measured daily, giving a mean  $^{176}\text{Hf}/^{177}\text{Hf}$  value of  $0.282681 \pm 33$  ( $2\sigma, n = 4$ ), which is in good agreement with the recommended mean  $^{176}\text{Hf}/^{177}\text{Hf}$  value of  $0.282680 \pm 31$  [56].

$\epsilon_{\text{Hf}}$ ,  $T$ , and  $f$  are defined in this study as follows:

$$\epsilon_{\text{Hf}}(0) = [({}^{176}\text{Hf}/{}^{177}\text{Hf})_S / ({}^{176}\text{Hf}/{}^{177}\text{Hf})_{\text{CHUR},0} - 1] \times 10,000,$$

$$\epsilon_{\text{Hf}}(t) = [({}^{176}\text{Hf}/{}^{177}\text{Hf})_S - ({}^{176}\text{Lu}/{}^{177}\text{Hf})_S \times (e^{\lambda t} - 1)] / [({}^{176}\text{Hf}/{}^{177}\text{Hf})_{\text{CHUR},0} - ({}^{176}\text{Lu}/{}^{177}\text{Hf})_{\text{CHUR}} \times (e^{\lambda t} - 1)] - 1] \times 10,000,$$

$$T_{\text{DM1}} = 1/\lambda \times \ln\{1 + [({}^{176}\text{Hf}/{}^{177}\text{Hf})_S - ({}^{176}\text{Hf}/{}^{177}\text{Hf})_{\text{DM}}] / [({}^{176}\text{Lu}/{}^{177}\text{Hf})_S - ({}^{176}\text{Lu}/{}^{177}\text{Hf})_{\text{DM}}]\},$$

$$T_{\text{DM2}} = T_{\text{DM1}} - (T_{\text{DM1}} - t) \times [(f_{\text{CC}} - f_S) / (f_{\text{CC}} - f_{\text{DM}})],$$

$$f_S = ({}^{176}\text{Lu}/{}^{177}\text{Hf})_S / ({}^{176}\text{Lu}/{}^{177}\text{Hf})_{\text{CHUR}} - 1,$$

$$f_{\text{CC}} = ({}^{176}\text{Lu}/{}^{177}\text{Hf})_{\text{C}} / ({}^{176}\text{Lu}/{}^{177}\text{Hf})_{\text{CHUR}} - 1, \text{ and}$$

$$f_{\text{DM}} = ({}^{176}\text{Lu}/{}^{177}\text{Hf})_{\text{DM}} / ({}^{176}\text{Lu}/{}^{177}\text{Hf})_{\text{CHUR}} - 1$$

where  $({}^{176}\text{Lu}/{}^{177}\text{Hf})_S$  and  $({}^{176}\text{Hf}/{}^{177}\text{Hf})_S$  are the sample measured values,  $({}^{176}\text{Lu}/{}^{177}\text{Hf})_{\text{CHUR}} = 0.0332$ ,  $({}^{176}\text{Hf}/{}^{177}\text{Hf})_{\text{CHUR},0} = 0.282772$ ,  $({}^{176}\text{Lu}/{}^{177}\text{Hf})_{\text{DM}} = 0.0384$ ,  $({}^{176}\text{Hf}/{}^{177}\text{Hf})_{\text{DM}} = 0.28325$  [59],  $({}^{176}\text{Lu}/{}^{177}\text{Hf})_{\text{C}} = 0.015$  [60],  $t$  is the formation time of the sample, and  $\lambda_{\text{Lu}} = 1.867 \times 10^{-11} \text{ yr}^{-1}$  [61].  $T_{\text{DM1}}$  and  $T_{\text{DM2}}$  are the single-stage Hf model and two-stage Hf model ages, respectively.  $f_{\text{CC}}$ ,  $f_S$ , and  $f_{\text{DM}}$  are the  $f_{\text{Lu/Hf}}$  values of the crustal source, sample, and depleted mantle, respectively.

#### 4. Analytical Results

The 200 detrital zircon grains have been subjected to U-Pb age dating, and the most concordant (>95%) results are listed in Table 1. The 186 concordant (>5%) detrital zircon grains have been analyzed for Hf isotopic data. The Lu-Hf isotope data are listed in Table 2. Representative zircon grain CL images and Th/U values are shown in Figures 4 and 5. The results are presented as a series of concordia diagrams (Figure 6). The probability density maps of ages are given in Figure 7. Hf isotope characteristics and U-Pb ages of detrital zircon grains are shown in Figures 8 and 9.

**Table 1.** LA-MC-ICP-MS U-Pb dating data for detrital zircons from the Chuanlinggou Formation.

No.	Conent (ppm)		Th/U	Isotopic Ratios						Age (Ma)						
	Th	U		$^{207}\text{Pb}/^{206}\text{Pb}$			$^{207}\text{Pb}/^{235}\text{U}$			$^{206}\text{Pb}/^{238}\text{U}$		$^{207}\text{Pb}/^{206}\text{Pb}$		$^{207}\text{Pb}/^{235}\text{U}$		
				1 Sigma	207	Pb/206	1 Sigma	207	Pb/235	1 Sigma	206	Pb/238	1 Sigma	207	Pb/206	1 Sigma
JJZ12-08																
1	27	36	0.75	0.1020	0.0007	4.0739	0.0445	0.2893	0.0024	1661	12	1649	9	1638	12	
2	18	22	0.84	0.1017	0.0007	3.9392	0.0534	0.2809	0.0035	1657	17	1622	11	1596	18	
3	29	55	0.53	0.1087	0.0006	4.5919	0.0399	0.3065	0.0022	1777	9	1748	7	1724	11	
4	77	110	0.70	0.1127	0.0006	4.9630	0.0454	0.3197	0.0027	1844	9	1813	8	1788	13	
5	22	30	0.72	0.1136	0.0010	5.2077	0.0818	0.3330	0.0049	1857	15	1854	13	1853	24	
7	79	130	0.61	0.1127	0.0009	4.9049	0.0545	0.3162	0.0028	1843	14	1803	9	1771	14	
8	73	119	0.62	0.1676	0.0011	10.6538	0.1263	0.4612	0.0044	2600	11	2493	11	2445	19	
9	54	110	0.49	0.1471	0.0013	8.4317	0.2111	0.4159	0.0096	2313	15	2279	23	2242	44	
10	59	83	0.70	0.1595	0.0014	9.7177	0.1270	0.4426	0.0045	2450	15	2408	12	2362	20	
11	87	159	0.55	0.1133	0.0014	5.1959	0.0984	0.3328	0.0040	1854	22	1852	16	1852	19	
12	48	58	0.83	0.1603	0.0017	10.1790	0.1378	0.4616	0.0036	2459	19	2451	13	2446	16	
14	29	119	0.24	0.0969	0.0010	3.4760	0.0884	0.2608	0.0063	1565	19	1522	20	1494	32	
15	185	206	0.89	0.1095	0.0010	4.8003	0.0875	0.3184	0.0051	1792	17	1785	15	1782	25	
16	118	186	0.63	0.1477	0.0015	9.2073	0.1283	0.4531	0.0042	2320	18	2359	13	2409	19	
17	32	39	0.81	0.1038	0.0017	4.2954	0.0917	0.3002	0.0037	1694	30	1693	18	1693	19	
18	72	75	0.97	0.1078	0.0027	4.6215	0.1666	0.3074	0.0040	1765	46	1753	30	1728	20	
19	91	74	1.23	0.1070	0.0024	4.6141	0.1394	0.3131	0.0051	1750	42	1752	25	1756	25	
20	29	122	0.24	0.1069	0.0016	4.4203	0.1112	0.3007	0.0069	1747	27	1716	21	1695	34	
21	84	72	1.17	0.1072	0.0022	4.4818	0.1323	0.3026	0.0042	1752	39	1728	25	1704	21	
22	100	77	1.29	0.1074	0.0021	4.4894	0.1257	0.3032	0.0055	1767	35	1729	23	1707	27	
23	60	126	0.48	0.1134	0.0024	5.1677	0.1370	0.3309	0.0051	1854	38	1847	23	1843	25	
24	123	190	0.65	0.1128	0.0034	4.8105	0.2675	0.3089	0.0079	1856	54	1787	47	1735	39	
25	136	99	1.38	0.1068	0.0018	4.4178	0.1083	0.2999	0.0049	1746	31	1716	20	1691	24	
26	47	34	1.37	0.1076	0.0014	4.4687	0.0898	0.3003	0.0038	1761	23	1725	17	1693	19	
27	184	153	1.21	0.1130	0.0017	5.1314	0.1384	0.3284	0.0061	1850	28	1841	23	1831	30	
28	130	82	1.59	0.1706	0.0029	11.4750	0.4184	0.4830	0.0104	2565	28	2563	34	2540	45	
29	202	191	1.06	0.1155	0.0011	5.4194	0.0923	0.3396	0.0047	1888	17	1888	15	1885	23	
30	94	67	1.40	0.1131	0.0013	5.0131	0.0601	0.3210	0.0022	1850	20	1822	10	1795	11	
31	65	40	1.62	0.1068	0.0024	4.2564	0.1065	0.2893	0.0097	1746	41	1685	21	1638	48	
32	66	63	1.06	0.1608	0.0013	10.3229	0.0871	0.4647	0.0022	2465	13	2464	8	2460	10	
33	220	146	1.51	0.1585	0.0010	10.3877	0.1868	0.4743	0.0077	2440	11	2470	17	2502	34	
34	46	36	1.26	0.1071	0.0008	4.5552	0.0545	0.3083	0.0033	1750	14	1741	10	1732	16	
36	85	76	1.13	0.1125	0.0016	5.0486	0.1121	0.3235	0.0036	1843	59	1828	19	1807	18	
37	161	97	1.67	0.1128	0.0015	5.0752	0.3772	0.3252	0.0204	1856	24	1832	63	1815	99	
38	52	53	0.98	0.1123	0.0019	4.8643	0.1106	0.3127	0.0039	1839	63	1796	19	1754	19	
39	69	72	0.95	0.1387	0.0019	7.8212	0.1502	0.4085	0.0058	2211	24	2211	17	2208	27	
40	134	169	0.79	0.1359	0.0010	7.5226	0.1014	0.4007	0.0045	2176	12	2176	12	2172	21	
41	123	61	2.01	0.1230	0.0016	6.0861	0.1606	0.3601	0.0097	2000	23	1988	23	1982	46	
42	231	218	1.06	0.1185	0.0025	5.7348	0.1758	0.3488	0.0057	1945	37	1937	27	1929	27	
43	35	46	0.77	0.1098	0.0014	4.7007	0.0833	0.3106	0.0051	1798	23	1767	15	1744	25	

**Table 1.** *Cont.*

No.	Content (ppm)		Th/U	Isotopic Ratios								Age (Ma)				
	Th	U		$^{207}\text{Pb}/^{206}\text{Pb}$	1 Sigma	$^{207}\text{Pb}/^{235}\text{U}$	1 Sigma	$^{206}\text{Pb}/^{238}\text{U}$	1 Sigma	$^{207}\text{Pb}/^{206}\text{Pb}$	1 Sigma	$^{207}\text{Pb}/^{235}\text{U}$	1 Sigma	$^{206}\text{Pb}/^{238}\text{U}$	1 Sigma	
JJZ12-08																
45	48	40	1.19	0.1086	0.0008	4.7488	0.0459	0.3170	0.0021	1776	15	1776	8	1775	11	
46	104	109	0.95	0.1205	0.0015	5.7963	0.1210	0.3457	0.0027	1965	22	1946	18	1914	13	
47	35	38	0.94	0.1461	0.0013	8.2482	0.1207	0.4090	0.0049	2302	15	2259	13	2210	23	
48	168	118	1.42	0.1744	0.0009	11.5079	0.0789	0.4778	0.0021	2611	9	2565	6	2518	9	
49	120	126	0.95	0.1193	0.0009	5.6854	0.0536	0.3453	0.0024	1946	13	1929	8	1912	11	
50	96	72	1.33	0.1668	0.0008	11.0026	0.0876	0.4784	0.0036	2526	42	2523	7	2520	16	
51	60	77	0.77	0.1441	0.0007	7.8826	0.1405	0.3964	0.0069	2277	8	2218	16	2153	32	
52	28	20	1.45	0.1134	0.0010	5.1375	0.1253	0.3279	0.0073	1855	16	1842	21	1828	36	
53	34	81	0.42	0.1161	0.0016	5.4746	0.0953	0.3411	0.0029	1898	25	1897	15	1892	14	
54	221	198	1.11	0.1153	0.0011	5.4113	0.0904	0.3398	0.0044	1887	-16	1887	14	1886	21	
55	78	103	0.76	0.1167	0.0021	5.5230	0.1333	0.3399	0.0026	1907	33	1904	21	1886	13	
56	64	87	0.73	0.1228	0.0013	6.1549	0.0853	0.3625	0.0033	1998	19	1998	12	1994	16	
57	26	41	0.63	0.1156	0.0015	5.3538	0.0809	0.3354	0.0032	1900	24	1878	13	1865	15	
58	28	28	1.00	0.1724	0.0014	11.3357	0.1600	0.4754	0.0053	2581	13	2551	13	2507	23	
59	32	46	0.68	0.1136	0.0012	5.1278	0.0840	0.3268	0.0042	1857	19	1841	14	1823	20	
60	29	26	1.14	0.1604	0.0014	9.8391	0.1345	0.4439	0.0050	2461	10	2420	13	2368	23	
61	155	169	0.92	0.1131	0.0008	4.9137	0.0642	0.3143	0.0035	1850	12	1805	11	1762	17	
62	29	35	0.84	0.1675	0.0013	11.0509	0.1592	0.4776	0.0063	2533	13	2527	13	2517	28	
63	5	8	0.69	0.1542	0.0030	9.1326	0.3802	0.4340	0.0184	2394	33	2351	38	2324	83	
64	147	110	1.34	0.1606	0.0010	10.2582	0.1470	0.4630	0.0066	2462	10	2458	13	2453	29	
65	24	36	0.66	0.1082	0.0010	4.5830	0.0659	0.3069	0.0037	1769	16	1746	12	1726	18	
66	29	70	0.42	0.1487	0.0011	8.5653	0.2470	0.4179	0.0126	2332	12	2293	26	2251	57	
67	226	156	1.45	0.1075	0.0016	4.6064	0.2718	0.3101	0.0169	1767	26	1750	49	1741	83	
68	17	15	1.11	0.1092	0.0011	4.8071	0.1437	0.3184	0.0085	1787	19	1786	25	1782	42	
69	288	220	1.31	0.1129	0.0011	5.0766	0.2014	0.3254	0.0104	1847	18	1832	34	1816	51	
70	43	44	0.97	0.1084	0.0010	4.6907	0.0719	0.3134	0.0040	1774	12	1766	13	1758	20	
71	561	124	4.52	0.1132	0.0010	5.0563	0.1124	0.3238	0.0068	1851	15	1829	19	1808	33	
72	53	73	0.73	0.1337	0.0013	7.2409	0.0882	0.3923	0.0027	2147	17	2142	11	2133	12	
73	215	154	1.39	0.1207	0.0015	5.8922	0.0820	0.3536	0.0019	1969	23	1960	12	1952	9	
74	52	34	1.50	0.1229	0.0009	6.0697	0.0782	0.3579	0.0038	1999	13	1986	11	1972	18	
75	110	49	2.26	0.1581	0.0021	10.3658	0.2754	0.4751	0.0110	2436	23	2468	25	2506	48	
76	191	146	1.31	0.1512	0.0012	8.9403	0.2431	0.4290	0.0117	2359	13	2332	25	2301	53	
77	44	41	1.07	0.1278	0.0038	6.4375	0.3047	0.3634	0.0092	2068	53	2037	42	1998	44	
78	124	81	1.54	0.1087	0.0015	4.7670	0.1073	0.3159	0.0034	1789	26	1779	19	1770	16	
79	77	98	0.78	0.1126	0.0013	5.0850	0.0746	0.3277	0.0036	1843	21	1834	13	1827	17	
80	92	194	0.48	0.1145	0.0014	5.3113	0.0751	0.3367	0.0032	1872	22	1871	12	1871	16	
81	271	113	2.39	0.1214	0.0013	5.8860	0.0755	0.3515	0.0031	1978	19	1959	11	1942	15	
82	80	62	1.29	0.1089	0.0010	4.7671	0.0514	0.3174	0.0023	1783	16	1779	9	1777	11	
83	215	160	1.34	0.1127	0.0012	4.9941	0.0569	0.3214	0.0024	1843	19	1818	10	1797	12	

Table 1. Cont.

No.	Conent (ppm)			Th/U	Isotopic Ratios						Age (Ma)					
	Th	U			$^{207}\text{Pb}/^{206}\text{Pb}$	1 Sigma	$^{207}\text{Pb}/^{235}\text{U}$	1 Sigma	$^{206}\text{Pb}/^{238}\text{U}$	1 Sigma	$^{207}\text{Pb}/^{206}\text{Pb}$	1 Sigma	$^{207}\text{Pb}/^{235}\text{U}$	1 Sigma	$^{206}\text{Pb}/^{238}\text{U}$	1 Sigma
JJZ12-08																
84	37	25	1.49	0.1032	0.0011	4.2273	0.0876	0.2967	0.0051	1683	20	1679	17	1675	25	
86	53	59	0.90	0.1100	0.0009	4.8650	0.0452	0.3206	0.0019	1799	15	1796	8	1793	9	
87	36	32	1.11	0.1131	0.0012	5.1092	0.0754	0.3272	0.0033	1850	19	1838	13	1825	16	
88	178	112	1.58	0.1608	0.0014	10.1890	0.1390	0.4586	0.0037	2465	15	2452	13	2434	17	
89	78	85	0.92	0.1164	0.0013	5.4359	0.0639	0.3389	0.0024	1902	22	1891	10	1881	12	
90	82	77	1.06	0.1166	0.0012	5.4477	0.0726	0.3378	0.0022	1906	20	1892	11	1876	10	
91	95	117	0.81	0.1589	0.0011	9.9387	0.0836	0.4529	0.0025	2444	13	2429	8	2408	11	
92	84	101	0.83	0.1134	0.0018	4.9649	0.0718	0.3179	0.0018	1855	28	1813	12	1779	9	
93	55	87	0.63	0.1721	0.0020	11.4809	0.1934	0.4823	0.0059	2589	20	2563	16	2537	26	
94	61	88	0.70	0.1588	0.0010	10.0174	0.0799	0.4571	0.0032	2443	11	2436	7	2427	14	
95	169	68	2.48	0.1225	0.0012	6.0397	0.0660	0.3572	0.0023	1994	19	1982	10	1969	11	
96	25	36	0.69	0.1064	0.0011	4.4991	0.0661	0.3062	0.0034	1739	23	1731	12	1722	17	
97	54	108	0.50	0.1130	0.0013	4.9741	0.0909	0.3184	0.0038	1850	21	1815	15	1782	19	
98	74	108	0.68	0.1134	0.0030	4.9893	0.1581	0.3184	0.0021	1854	48	1818	27	1782	10	
100	98	149	0.66	0.1075	0.0012	4.6069	0.0625	0.3099	0.0022	1758	26	1751	11	1740	11	
PJB12-11																
1	100	88	1.14	0.1659	0.0024	10.8250	0.3894	0.4733	0.0167	2517	25	2508	33	2498	73	
2	161	140	1.16	0.1521	0.0011	9.2108	0.2469	0.4391	0.0122	2369	13	2359	25	2347	55	
3	74	66	1.12	0.1523	0.0017	9.0768	0.2798	0.4318	0.0125	2373	19	2346	28	2314	56	
4	60	44	1.35	0.1072	0.0010	4.4307	0.0785	0.2998	0.0047	1754	17	1718	15	1691	23	
5	14	48	0.29	0.1693	0.0030	10.8239	0.3976	0.4635	0.0154	2550	30	2508	34	2455	68	
6	95	76	1.25	0.1539	0.0012	9.3889	0.4350	0.4421	0.0202	2391	14	2377	43	2360	91	
7	124	199	0.62	0.1533	0.0008	9.1127	0.0918	0.4309	0.0036	2383	9	2349	9	2310	16	
8	21	15	1.40	0.1077	0.0016	4.6431	0.1748	0.3132	0.0110	1761	27	1757	32	1757	54	
9	41	30	1.39	0.1157	0.0016	5.3671	0.1016	0.3364	0.0044	1890	26	1880	16	1870	21	
10	158	106	1.49	0.1603	0.0012	10.2262	0.1638	0.4629	0.0065	2458	8	2456	15	2452	29	
11	109	79	1.37	0.1232	0.0009	6.0970	0.0756	0.3590	0.0037	2003	13	1990	11	1978	18	
12	93	127	0.73	0.1681	0.0015	10.9648	0.2870	0.4732	0.0122	2539	15	2520	24	2498	54	
13	22	21	1.08	0.1135	0.0016	5.1324	0.1534	0.3281	0.0084	1855	26	1842	25	1829	41	
14	64	108	0.59	0.1591	0.0008	9.9890	0.1173	0.4554	0.0049	2446	8	2434	11	2419	22	
15	33	76	0.43	0.1236	0.0009	5.9971	0.0866	0.3512	0.0041	2010	18	1975	13	1940	20	
17	63	100	0.63	0.1451	0.0007	8.4193	0.1299	0.4211	0.0066	2289	9	2277	14	2266	30	
18	319	268	1.19	0.1589	0.0009	9.9461	0.2881	0.4535	0.0121	2444	9	2430	27	2411	54	
19	280	349	0.80	0.1589	0.0009	9.8781	0.4572	0.4507	0.0228	2444	10	2424	43	2398	101	
20	199	206	0.97	0.1120	0.0021	4.7783	0.1638	0.3108	0.0151	1831	34	1781	29	1745	74	
21	164	177	0.93	0.1209	0.0016	5.9309	0.1671	0.3551	0.0085	1969	23	1966	25	1959	40	
22	132	100	1.31	0.1139	0.0010	5.2600	0.0733	0.3345	0.0037	1863	15	1862	12	1860	18	
23	192	96	2.00	0.1164	0.0008	5.4966	0.0937	0.3420	0.0053	1902	8	1900	15	1896	26	

**Table 1.** *Cont.*

No.	Content (ppm)		Th/U	Isotopic Ratios						Age (Ma)					
	Th	U		$^{207}\text{Pb}/^{206}\text{Pb}$	1 Sigma	$^{207}\text{Pb}/^{235}\text{U}$	1 Sigma	$^{206}\text{Pb}/^{238}\text{U}$	1 Sigma	$^{207}\text{Pb}/^{206}\text{Pb}$	1 Sigma	$^{207}\text{Pb}/^{235}\text{U}$	1 Sigma	$^{206}\text{Pb}/^{238}\text{U}$	1 Sigma
PJBJ12-11															
24	32	40	0.80	0.1070	0.0008	4.4659	0.0603	0.3024	0.0035	1750	13	1725	11	1703	17
25	125	92	1.35	0.1355	0.0006	7.4712	0.0722	0.3994	0.0036	2172	8	2170	9	2166	17
26	104	69	1.50	0.1586	0.0012	9.9910	0.1284	0.4560	0.0047	2443	12	2434	12	2422	21
27	70	78	0.89	0.1297	0.0008	6.6749	0.0623	0.3730	0.0030	2094	11	2069	8	2043	14
28	98	95	1.03	0.1594	0.0011	10.0482	0.1935	0.4563	0.0082	2450	11	2439	18	2423	36
30	45	46	0.98	0.1066	0.0011	4.5136	0.0589	0.3061	0.0023	1743	19	1734	11	1722	12
31	44	36	1.22	0.1072	0.0011	4.4099	0.0531	0.2981	0.0025	1752	18	1714	10	1682	12
32	175	65	2.70	0.1124	0.0013	5.0722	0.0668	0.3264	0.0018	1839	21	1832	11	1821	9
33	198	152	1.30	0.2382	0.0013	20.2304	0.1694	0.6148	0.0041	3109	9	3102	8	3089	16
34	106	119	0.89	0.1467	0.0008	8.7070	0.0558	0.4299	0.0021	2309	10	2308	6	2305	10
35	223	160	1.40	0.1121	0.0009	5.0522	0.0399	0.3268	0.0016	1833	13	1828	7	1823	8
36	33	23	1.41	0.1072	0.0010	4.4362	0.0734	0.2999	0.0045	1754	17	1719	14	1691	22
37	94	109	0.86	0.1239	0.0011	6.1353	0.0630	0.3587	0.0022	2013	15	1995	9	1976	10
38	91	67	1.35	0.1164	0.0010	5.4788	0.0569	0.3408	0.0020	1902	15	1897	9	1891	10
40	34	41	0.83	0.1450	0.0013	8.1009	0.1794	0.4041	0.0074	2287	15	2242	20	2188	34
41	106	177	0.60	0.1511	0.0008	9.1603	0.0845	0.4387	0.0028	2358	9	2354	8	2345	13
42	148	135	1.09	0.1607	0.0011	10.3059	0.0953	0.4645	0.0025	2463	13	2463	9	2459	11
43	69	105	0.66	0.1597	0.0013	10.1450	0.1043	0.4598	0.0027	2454	13	2448	10	2439	12
44	93	108	0.86	0.1591	0.0012	9.8819	0.0883	0.4500	0.0030	2447	12	2424	8	2395	14
46	35	39	0.90	0.1668	0.0015	10.6331	0.1157	0.4619	0.0033	2528	16	2492	10	2448	15
47	44	26	1.71	0.1543	0.0016	9.4427	0.1304	0.4437	0.0045	2394	18	2382	13	2367	20
48	101	99	1.02	0.1618	0.0019	10.4511	0.2871	0.4667	0.0085	2476	20	2476	26	2469	37
49	98	95	1.03	0.1226	0.0018	6.1028	0.1083	0.3607	0.0033	1994	26	1991	16	1985	16
51	74	91	0.81	0.1075	0.0019	4.5797	0.1343	0.3075	0.0059	1758	33	1746	24	1729	29
53	128	87	1.47	0.1701	0.0054	11.3690	1.0457	0.4747	0.0308	2558	52	2554	86	2504	135
54	153	150	1.02	0.1690	0.0024	11.2108	0.4001	0.4811	0.0170	2548	24	2541	33	2532	74
55	99	90	1.10	0.1179	0.0019	5.5464	0.1144	0.3407	0.0040	1924	30	1908	18	1890	19
56	99	72	1.37	0.1126	0.0021	4.8900	0.1192	0.3147	0.0047	1843	33	1801	21	1764	23
57	78	74	1.04	0.1133	0.0019	5.2016	0.1143	0.3320	0.0043	1854	25	1853	19	1848	21
58	175	128	1.37	0.1538	0.0007	9.2458	0.1510	0.4358	0.0070	2388	8	2363	15	2332	31
59	83	63	1.31	0.1530	0.0014	9.2403	0.1402	0.4379	0.0057	2380	15	2362	14	2341	26
60	50	52	0.96	0.1067	0.0012	4.5207	0.0954	0.3066	0.0053	1743	22	1735	18	1724	26
61	77	126	0.61	0.1524	0.0026	9.3663	0.6560	0.4440	0.0270	2373	29	2375	64	2369	121
63	91	103	0.88	0.1501	0.0011	8.8502	0.2574	0.4271	0.0117	2347	13	2323	27	2293	53
64	24	10	2.41	0.1218	0.0062	5.4772	0.1647	0.3380	0.0098	1984	86	1897	26	1877	47
65	208	116	1.79	0.1560	0.0009	9.6819	0.4641	0.4499	0.0223	2413	16	2405	44	2395	99
66	97	138	0.71	0.1586	0.0010	9.8606	0.1583	0.4505	0.0068	2443	10	2422	15	2398	30
67	38	135	0.28	0.1135	0.0016	5.1890	0.1357	0.3310	0.0072	1857	26	1851	22	1843	35
68	33	38	0.87	0.1071	0.0012	4.5542	0.0581	0.3084	0.0022	1750	22	1741	11	1733	11

**Table 1.** *Cont.*

No.	Conent (ppm)		Th/U	Isotopic Ratios								Age (Ma)				
	Th	U		$^{207}\text{Pb}/^{206}\text{Pb}$	1 Sigma	$^{207}\text{Pb}/^{235}\text{U}$	1 Sigma	$^{206}\text{Pb}/^{238}\text{U}$	1 Sigma	$^{207}\text{Pb}/^{206}\text{Pb}$	1 Sigma	$^{207}\text{Pb}/^{235}\text{U}$	1 Sigma	$^{206}\text{Pb}/^{238}\text{U}$	1 Sigma	
PJBJ12-11																
69	87	132	0.65	0.1129	0.0013	4.9428	0.0622	0.3171	0.0018	1856	55	1810	11	1776	9	
70	16	193	0.09	0.1438	0.0013	7.9142	0.0831	0.3982	0.0021	2273	22	2221	10	2161	10	
71	32	37	0.88	0.1728	0.0031	11.5599	0.5171	0.4832	0.0173	2587	31	2569	42	2541	75	
72	145	64	2.25	0.1595	0.0022	10.1240	0.2546	0.4607	0.0141	2450	23	2446	23	2442	62	
73	226	121	1.87	0.1582	0.0017	10.0108	0.1674	0.4580	0.0057	2437	18	2436	15	2431	25	
74	112	88	1.28	0.1151	0.0011	5.3223	0.0743	0.3345	0.0033	1883	17	1873	12	1860	16	
75	95	85	1.12	0.2280	0.0015	18.7653	0.2371	0.5962	0.0068	3038	11	3030	12	3015	28	
76	94	47	2.02	0.1579	0.0012	9.7923	0.1422	0.4488	0.0054	2435	13	2415	13	2390	24	
77	169	241	0.70	0.1538	0.0009	9.4554	0.1502	0.4452	0.0066	2389	5	2383	15	2374	29	
78	26	18	1.44	0.1080	0.0011	4.3605	0.0899	0.2929	0.0057	1766	19	1705	17	1656	29	
79	152	139	1.10	0.1123	0.0011	5.0301	0.0656	0.3252	0.0038	1836	17	1824	11	1815	18	
80	33	39	0.85	0.1068	0.0008	4.5407	0.0540	0.3085	0.0034	1746	14	1739	10	1733	17	
81	27	22	1.24	0.1078	0.0008	4.6187	0.0897	0.3104	0.0057	1763	13	1753	16	1743	28	
82	49	57	0.87	0.1124	0.0011	4.7773	0.0710	0.3076	0.0030	1839	19	1781	13	1729	15	
83	98	61	1.61	0.1068	0.0008	4.5527	0.0426	0.3093	0.0024	1746	14	1741	8	1738	12	
84	115	165	0.70	0.1607	0.0010	10.2960	0.1003	0.4640	0.0033	2465	10	2462	9	2457	15	
85	56	58	0.97	0.1131	0.0014	5.0517	0.0749	0.3231	0.0018	1850	22	1828	13	1805	9	
86	87	53	1.64	0.1260	0.0010	6.3753	0.0621	0.3668	0.0024	2043	14	2029	9	2014	11	
87	90	224	0.40	0.1126	0.0011	5.1336	0.0586	0.3305	0.0021	1843	13	1842	10	1841	10	
88	128	117	1.09	0.1686	0.0020	11.1488	0.1921	0.4779	0.0039	2544	20	2536	16	2518	17	
89	108	108	1.00	0.1629	0.0019	10.5746	0.1816	0.4694	0.0040	2487	20	2487	16	2481	18	
90	41	57	0.71	0.1142	0.0012	5.2394	0.0614	0.3328	0.0021	1933	17	1859	10	1852	10	
92	73	85	0.86	0.1700	0.0010	11.4092	0.0855	0.4867	0.0027	2558	10	2557	7	2557	12	
93	57	79	0.73	0.1704	0.0010	11.3359	0.0965	0.4821	0.0031	2561	10	2551	8	2537	14	
94	79	63	1.25	0.1698	0.0027	11.3223	0.2297	0.4833	0.0067	2555	27	2550	19	2542	29	
95	6	82	0.07	0.0884	0.0012	2.8745	0.0878	0.2338	0.0057	1391	26	1375	23	1355	30	
96	29	28	1.07	0.1073	0.0011	4.5792	0.0603	0.3093	0.0028	1754	18	1746	11	1737	14	
97	110	111	0.99	0.1473	0.0009	7.2872	0.0812	0.3585	0.0038	2315	10	2147	10	1975	18	
98	48	42	1.16	0.1359	0.0013	7.3201	0.0776	0.3903	0.0024	2176	17	2151	10	2124	11	
99	43	39	1.11	0.1777	0.0015	12.2345	0.1285	0.4984	0.0033	2631	19	2623	10	2607	14	
100	88	48	1.81	0.1688	0.0023	10.7511	0.2861	0.4608	0.0078	2545	24	2502	25	2443	35	

**Table 2.** In situ Lu-Hf isotopes analytical data for detrital zircons from the Chuanlinggou Formation.

No.	Conent (ppm)			Th/U	Isotopic Ratios						Age (Ma)						
	Th	U			$^{207}\text{Pb}/^{206}\text{Pb}$	1 Sigma	$^{207}\text{Pb}/^{235}\text{U}$	1 Sigma	$^{206}\text{Pb}/^{238}\text{U}$	1 Sigma	$^{207}\text{Pb}/^{206}\text{Pb}$	1 Sigma	$^{207}\text{Pb}/^{235}\text{U}$	1 Sigma	$^{206}\text{Pb}/^{238}\text{U}$	1 Sigma	
JJZ12-08																	
1	27	36	0.75	0.1020	0.0007	4.0739	0.0445	0.2893	0.0024	1661	12	1649	9	1638	12		
2	18	22	0.84	0.1017	0.0007	3.9392	0.0534	0.2809	0.0035	1657	17	1622	11	1596	18		
3	29	55	0.53	0.1087	0.0006	4.5919	0.0399	0.3065	0.0022	1777	9	1748	7	1724	11		
4	77	110	0.70	0.1127	0.0006	4.9630	0.0454	0.3197	0.0027	1844	9	1813	8	1788	13		
5	22	30	0.72	0.1136	0.0010	5.2077	0.0818	0.3330	0.0049	1857	15	1854	13	1853	24		
7	79	130	0.61	0.1127	0.0009	4.9049	0.0545	0.3162	0.0028	1843	14	1803	9	1771	14		
8	73	119	0.62	0.1676	0.0011	10.6538	0.1263	0.4612	0.0044	2600	11	2493	11	2445	19		
9	54	110	0.49	0.1471	0.0013	8.4317	0.2111	0.4159	0.0096	2313	15	2279	23	2242	44		
10	59	83	0.70	0.1595	0.0014	9.7177	0.1270	0.4426	0.0045	2450	15	2408	12	2362	20		
11	87	159	0.55	0.1133	0.0014	5.1959	0.0984	0.3328	0.0040	1854	22	1852	16	1852	19		
12	48	58	0.83	0.1603	0.0017	10.1790	0.1378	0.4616	0.0036	2459	19	2451	13	2446	16		
14	29	119	0.24	0.0969	0.0010	3.4760	0.0884	0.2608	0.0063	1565	19	1522	20	1494	32		
15	185	206	0.89	0.1095	0.0010	4.8003	0.0875	0.3184	0.0051	1792	17	1785	15	1782	25		
16	118	186	0.63	0.1477	0.0015	9.2073	0.1283	0.4531	0.0042	2320	18	2359	13	2409	19		
17	32	39	0.81	0.1038	0.0017	4.2954	0.0917	0.3002	0.0037	1694	30	1693	18	1693	19		
18	72	75	0.97	0.1078	0.0027	4.6215	0.1666	0.3074	0.0040	1765	46	1753	30	1728	20		
19	91	74	1.23	0.1070	0.0024	4.6141	0.1394	0.3131	0.0051	1750	42	1752	25	1756	25		
20	29	122	0.24	0.1069	0.0016	4.4203	0.1112	0.3007	0.0069	1747	27	1716	21	1695	34		
21	84	72	1.17	0.1072	0.0022	4.4818	0.1323	0.3026	0.0042	1752	39	1728	25	1704	21		
22	100	77	1.29	0.1074	0.0021	4.4894	0.1257	0.3032	0.0055	1767	35	1729	23	1707	27		
23	60	126	0.48	0.1134	0.0024	5.1677	0.1370	0.3309	0.0051	1854	38	1847	23	1843	25		
24	123	190	0.65	0.1128	0.0034	4.8105	0.2675	0.3089	0.0079	1856	54	1787	47	1735	39		
25	136	99	1.38	0.1068	0.0018	4.4178	0.1083	0.2999	0.0049	1746	31	1716	20	1691	24		
26	47	34	1.37	0.1076	0.0014	4.4687	0.0898	0.3003	0.0038	1761	23	1725	17	1693	19		
27	184	153	1.21	0.1130	0.0017	5.1314	0.1384	0.3284	0.0061	1850	28	1841	23	1831	30		
28	130	82	1.59	0.1706	0.0029	11.4750	0.4184	0.4830	0.0104	2565	28	2563	34	2540	45		
29	202	191	1.06	0.1155	0.0011	5.4194	0.0923	0.3396	0.0047	1888	17	1888	15	1885	23		
30	94	67	1.40	0.1131	0.0013	5.0131	0.0601	0.3210	0.0022	1850	20	1822	10	1795	11		
31	65	40	1.62	0.1068	0.0024	4.2564	0.1065	0.2893	0.0097	1746	41	1685	21	1638	48		
32	66	63	1.06	0.1608	0.0013	10.3229	0.0871	0.4647	0.0022	2465	13	2464	8	2460	10		
33	220	146	1.51	0.1585	0.0010	10.3877	0.1868	0.4743	0.0077	2440	11	2470	17	2502	34		
34	46	36	1.26	0.1071	0.0008	4.5552	0.0545	0.3083	0.0033	1750	14	1741	10	1732	16		
36	85	76	1.13	0.1125	0.0016	5.0486	0.1121	0.3235	0.0036	1843	59	1828	19	1807	18		
37	161	97	1.67	0.1128	0.0015	5.0752	0.3772	0.3252	0.0204	1856	24	1832	63	1815	99		
38	52	53	0.98	0.1123	0.0019	4.8643	0.1106	0.3127	0.0039	1839	63	1796	19	1754	19		
39	69	72	0.95	0.1387	0.0019	7.8212	0.1502	0.4085	0.0058	2211	24	2211	17	2208	27		
40	134	169	0.79	0.1359	0.0010	7.5226	0.1014	0.4007	0.0045	2176	12	2176	12	2172	21		
41	123	61	2.01	0.1230	0.0016	6.0861	0.1606	0.3601	0.0097	2000	23	1988	23	1982	46		
42	231	218	1.06	0.1185	0.0025	5.7348	0.1758	0.3488	0.0057	1945	37	1937	27	1929	27		
43	35	46	0.77	0.1098	0.0014	4.7007	0.0833	0.3106	0.0051	1798	23	1767	15	1744	25		
45	48	40	1.19	0.1086	0.0008	4.7488	0.0459	0.3170	0.0021	1776	15	1776	8	1775	11		

**Table 2.** *Cont.*

No.	Conent (ppm)		Th/U	Isotopic Ratios						Age (Ma)					
	Th	U		$^{207}\text{Pb}/^{206}\text{Pb}$	1 Sigma	$^{207}\text{Pb}/^{235}\text{U}$	1 Sigma	$^{206}\text{Pb}/^{238}\text{U}$	1 Sigma	$^{207}\text{Pb}/^{206}\text{Pb}$	1 Sigma	$^{207}\text{Pb}/^{235}\text{U}$	1 Sigma	$^{206}\text{Pb}/^{238}\text{U}$	1 Sigma
JJZ12-08															
46	104	109	0.95	0.1205	0.0015	5.7963	0.1210	0.3457	0.0027	1965	22	1946	18	1914	13
47	35	38	0.94	0.1461	0.0013	8.2482	0.1207	0.4090	0.0049	2302	15	2259	13	2210	23
48	168	118	1.42	0.1744	0.0009	11.5079	0.0789	0.4778	0.0021	2611	9	2565	6	2518	9
49	120	126	0.95	0.1193	0.0009	5.6854	0.0536	0.3453	0.0024	1946	13	1929	8	1912	11
50	96	72	1.33	0.1668	0.0008	11.0026	0.0876	0.4784	0.0036	2526	42	2523	7	2520	16
51	60	77	0.77	0.1441	0.0007	7.8826	0.1405	0.3964	0.0069	2277	8	2218	16	2153	32
52	28	20	1.45	0.1134	0.0010	5.1375	0.1253	0.3279	0.0073	1855	16	1842	21	1828	36
53	34	81	0.42	0.1161	0.0016	5.4746	0.0953	0.3411	0.0029	1898	25	1897	15	1892	14
54	221	198	1.11	0.1153	0.0011	5.4113	0.0904	0.3398	0.0044	1887	-16	1887	14	1886	21
55	78	103	0.76	0.1167	0.0021	5.5230	0.1333	0.3399	0.0026	1907	33	1904	21	1886	13
56	64	87	0.73	0.1228	0.0013	6.1549	0.0853	0.3625	0.0033	1998	19	1998	12	1994	16
57	26	41	0.63	0.1156	0.0015	5.3538	0.0809	0.3354	0.0032	1900	24	1878	13	1865	15
58	28	28	1.00	0.1724	0.0014	11.3357	0.1600	0.4754	0.0053	2581	13	2551	13	2507	23
59	32	46	0.68	0.1136	0.0012	5.1278	0.0840	0.3268	0.0042	1857	19	1841	14	1823	20
60	29	26	1.14	0.1604	0.0014	9.8391	0.1345	0.4439	0.0050	2461	10	2420	13	2368	23
61	155	169	0.92	0.1131	0.0008	4.9137	0.0642	0.3143	0.0035	1850	12	1805	11	1762	17
62	29	35	0.84	0.1675	0.0013	11.0509	0.1592	0.4776	0.0063	2533	13	2527	13	2517	28
63	5	8	0.69	0.1542	0.0030	9.1326	0.3802	0.4340	0.0184	2394	33	2351	38	2324	83
64	147	110	1.34	0.1606	0.0010	10.2582	0.1470	0.4630	0.0066	2462	10	2458	13	2453	29
65	24	36	0.66	0.1082	0.0010	4.5830	0.0659	0.3069	0.0037	1769	16	1746	12	1726	18
66	29	70	0.42	0.1487	0.0011	8.5653	0.2470	0.4179	0.0126	2332	12	2293	26	2251	57
67	226	156	1.45	0.1075	0.0016	4.6064	0.2718	0.3101	0.0169	1767	26	1750	49	1741	83
68	17	15	1.11	0.1092	0.0011	4.8071	0.1437	0.3184	0.0085	1787	19	1786	25	1782	42
69	288	220	1.31	0.1129	0.0011	5.0766	0.2014	0.3254	0.0104	1847	18	1832	34	1816	51
70	43	44	0.97	0.1084	0.0010	4.6907	0.0719	0.3134	0.0040	1774	12	1766	13	1758	20
71	561	124	4.52	0.1132	0.0010	5.0563	0.1124	0.3238	0.0068	1851	15	1829	19	1808	33
72	53	73	0.73	0.1337	0.0013	7.2409	0.0882	0.3923	0.0027	2147	17	2142	11	2133	12
73	215	154	1.39	0.1207	0.0015	5.8922	0.0820	0.3536	0.0019	1969	23	1960	12	1952	9
74	52	34	1.50	0.1229	0.0009	6.0697	0.0782	0.3579	0.0038	1999	13	1986	11	1972	18
75	110	49	2.26	0.1581	0.0021	10.3658	0.2754	0.4751	0.0110	2436	23	2468	25	2506	48
76	191	146	1.31	0.1512	0.0012	8.9403	0.2431	0.4290	0.0117	2359	13	2332	25	2301	53
77	44	41	1.07	0.1278	0.0038	6.4375	0.3047	0.3634	0.0092	2068	53	2037	42	1998	44
78	124	81	1.54	0.1087	0.0015	4.7670	0.1073	0.3159	0.0034	1789	26	1779	19	1770	16
79	77	98	0.78	0.1126	0.0013	5.0850	0.0746	0.3277	0.0036	1843	21	1834	13	1827	17
80	92	194	0.48	0.1145	0.0014	5.3113	0.0751	0.3367	0.0032	1872	22	1871	12	1871	16
81	271	113	2.39	0.1214	0.0013	5.8860	0.0755	0.3515	0.0031	1978	19	1959	11	1942	15
82	80	62	1.29	0.1089	0.0010	4.7671	0.0514	0.3174	0.0023	1783	16	1779	9	1777	11
83	215	160	1.34	0.1127	0.0012	4.9941	0.0569	0.3214	0.0024	1843	19	1818	10	1797	12
84	37	25	1.49	0.1032	0.0011	4.2273	0.0876	0.2967	0.0051	1683	20	1679	17	1675	25

Table 2. Cont.

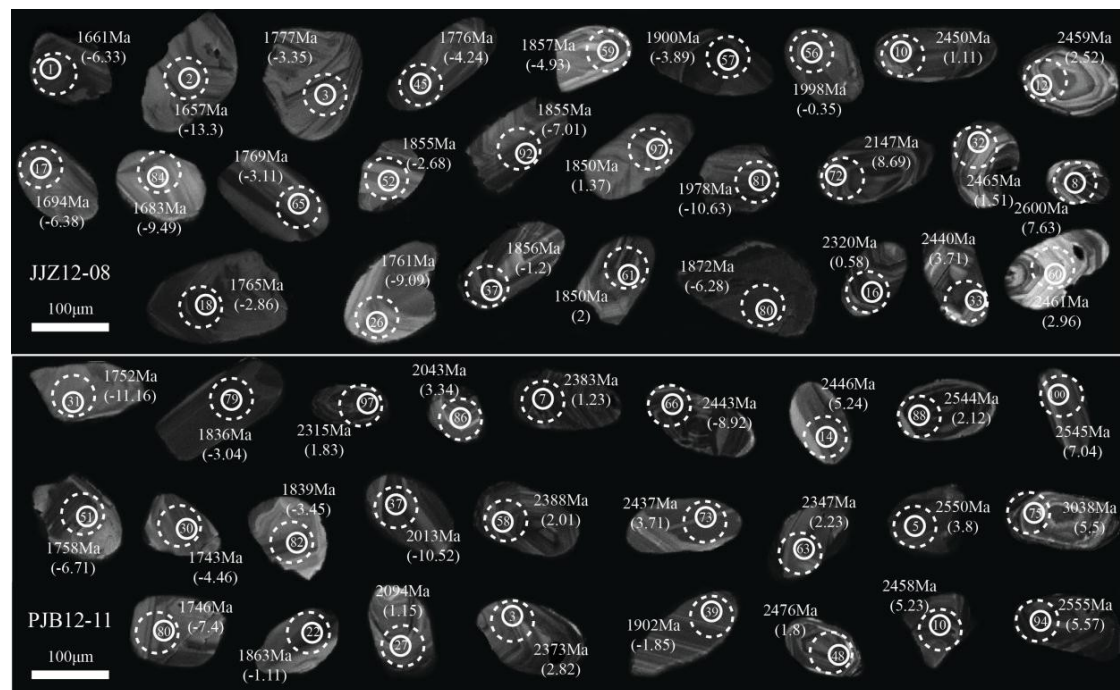
No.	Conent (ppm)			Th/U	Isotopic Ratios						Age (Ma)						
	Th	U			$^{207}\text{Pb}/^{206}\text{Pb}$	1 Sigma	$^{207}\text{Pb}/^{235}\text{U}$	1 Sigma	$^{206}\text{Pb}/^{238}\text{U}$	1 Sigma	$^{207}\text{Pb}/^{206}\text{Pb}$	1 Sigma	$^{207}\text{Pb}/^{235}\text{U}$	1 Sigma	$^{206}\text{Pb}/^{238}\text{U}$	1 Sigma	
JJZ12-08																	
86	53	59	0.90	0.1100	0.0009	4.8650	0.0452	0.3206	0.0019	1799	15	1796	8	1793	9		
87	36	32	1.11	0.1131	0.0012	5.1092	0.0754	0.3272	0.0033	1850	19	1838	13	1825	16		
88	178	112	1.58	0.1608	0.0014	10.1890	0.1390	0.4586	0.0037	2465	15	2452	13	2434	17		
89	78	85	0.92	0.1164	0.0013	5.4359	0.0639	0.3389	0.0024	1902	22	1891	10	1881	12		
90	82	77	1.06	0.1166	0.0012	5.4477	0.0726	0.3378	0.0022	1906	20	1892	11	1876	10		
91	95	117	0.81	0.1589	0.0011	9.9387	0.0836	0.4529	0.0025	2444	13	2429	8	2408	11		
92	84	101	0.83	0.1134	0.0018	4.9649	0.0718	0.3179	0.0018	1855	28	1813	12	1779	9		
93	55	87	0.63	0.1721	0.0020	11.4809	0.1934	0.4823	0.0059	2589	20	2563	16	2537	26		
94	61	88	0.70	0.1588	0.0010	10.0174	0.0799	0.4571	0.0032	2443	11	2436	7	2427	14		
95	169	68	2.48	0.1225	0.0012	6.0397	0.0660	0.3572	0.0023	1994	19	1982	10	1969	11		
96	25	36	0.69	0.1064	0.0011	4.4991	0.0661	0.3062	0.0034	1739	23	1731	12	1722	17		
97	54	108	0.50	0.1130	0.0013	4.9741	0.0909	0.3184	0.0038	1850	21	1815	15	1782	19		
98	74	108	0.68	0.1134	0.0030	4.9893	0.1581	0.3184	0.0021	1854	48	1818	27	1782	10		
100	98	149	0.66	0.1075	0.0012	4.6069	0.0625	0.3099	0.0022	1758	26	1751	11	1740	11		
PJB12-11																	
1	100	88	1.14	0.1659	0.0024	10.8250	0.3894	0.4733	0.0167	2517	25	2508	33	2498	73		
2	161	140	1.16	0.1521	0.0011	9.2108	0.2469	0.4391	0.0122	2369	13	2359	25	2347	55		
3	74	66	1.12	0.1523	0.0017	9.0768	0.2798	0.4318	0.0125	2373	19	2346	28	2314	56		
4	60	44	1.35	0.1072	0.0010	4.4307	0.0785	0.2998	0.0047	1754	17	1718	15	1691	23		
5	14	48	0.29	0.1693	0.0030	10.8239	0.3976	0.4635	0.0154	2550	30	2508	34	2455	68		
6	95	76	1.25	0.1539	0.0012	9.3889	0.4350	0.4421	0.0202	2391	14	2377	43	2360	91		
7	124	199	0.62	0.1533	0.0008	9.1127	0.0918	0.4309	0.0036	2383	9	2349	9	2310	16		
8	21	15	1.40	0.1077	0.0016	4.6431	0.1748	0.3132	0.0110	1761	27	1757	32	1757	54		
9	41	30	1.39	0.1157	0.0016	5.3671	0.1016	0.3364	0.0044	1890	26	1880	16	1870	21		
10	158	106	1.49	0.1603	0.0012	10.2262	0.1638	0.4629	0.0065	2458	8	2456	15	2452	29		
11	109	79	1.37	0.1232	0.0009	6.0970	0.0756	0.3590	0.0037	2003	13	1990	11	1978	18		
12	93	127	0.73	0.1681	0.0015	10.9648	0.2870	0.4732	0.0122	2539	15	2520	24	2498	54		
13	22	21	1.08	0.1135	0.0016	5.1324	0.1534	0.3281	0.0084	1855	26	1842	25	1829	41		
14	64	108	0.59	0.1591	0.0008	9.9890	0.1173	0.4554	0.0049	2446	8	2434	11	2419	22		
15	33	76	0.43	0.1236	0.0009	5.9971	0.0866	0.3512	0.0041	2010	18	1975	13	1940	20		
17	63	100	0.63	0.1451	0.0007	8.4193	0.1299	0.4211	0.0066	2289	9	2277	14	2266	30		
18	319	268	1.19	0.1589	0.0009	9.9461	0.2881	0.4535	0.0121	2444	9	2430	27	2411	54		
19	280	349	0.80	0.1589	0.0009	9.8781	0.4572	0.4507	0.0228	2444	10	2424	43	2398	101		
20	199	206	0.97	0.1120	0.0021	4.7783	0.1638	0.3108	0.0151	1831	34	1781	29	1745	74		
21	164	177	0.93	0.1209	0.0016	5.9309	0.1671	0.3551	0.0085	1969	23	1966	25	1959	40		
22	132	100	1.31	0.1139	0.0010	5.2600	0.0733	0.3345	0.0037	1863	15	1862	12	1860	18		
23	192	96	2.00	0.1164	0.0008	5.4966	0.0937	0.3420	0.0053	1902	8	1900	15	1896	26		
24	32	40	0.80	0.1070	0.0008	4.4659	0.0603	0.3024	0.0035	1750	13	1725	11	1703	17		
25	125	92	1.35	0.1355	0.0006	7.4712	0.0722	0.3994	0.0036	2172	8	2170	9	2166	17		
26	104	69	1.50	0.1586	0.0012	9.9910	0.1284	0.4560	0.0047	2443	12	2434	12	2422	21		

**Table 2.** *Cont.*

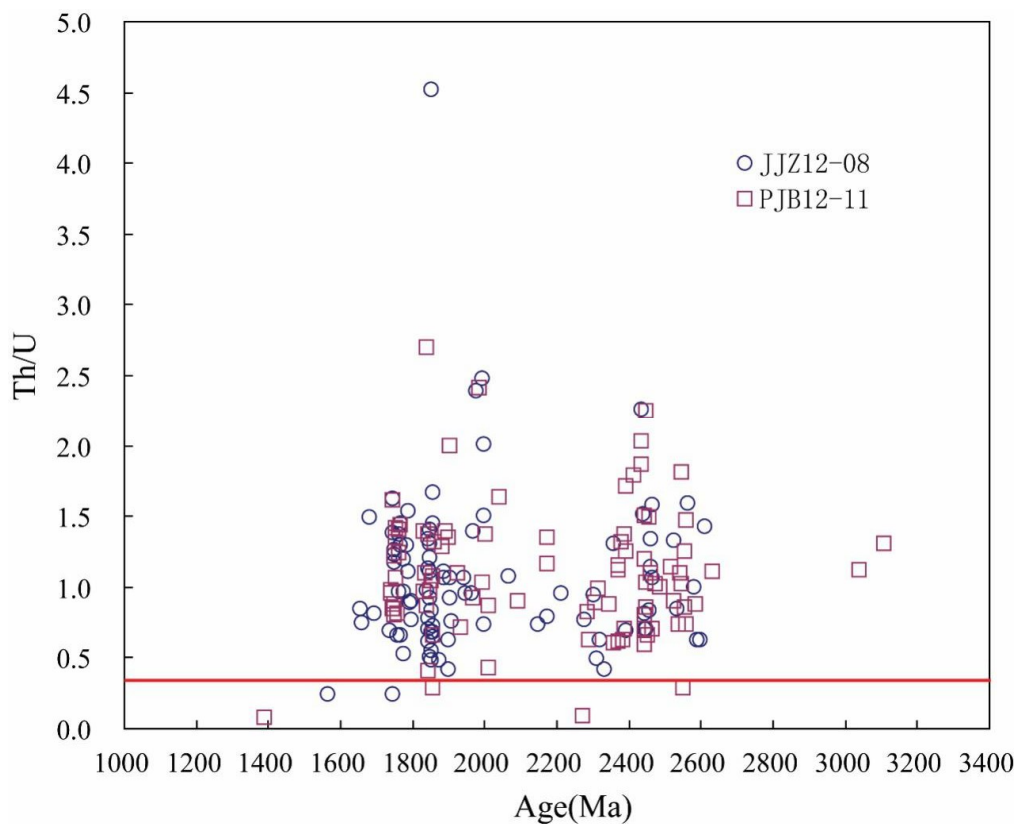
No.	Content (ppm)		Th/U	Isotopic Ratios								Age (Ma)				
	Th	U		$^{207}\text{Pb}/^{206}\text{Pb}$	1 Sigma	$^{207}\text{Pb}/^{235}\text{U}$	1 Sigma	$^{206}\text{Pb}/^{238}\text{U}$	1 Sigma	$^{207}\text{Pb}/^{206}\text{Pb}$	1 Sigma	$^{207}\text{Pb}/^{235}\text{U}$	1 Sigma	$^{206}\text{Pb}/^{238}\text{U}$	1 Sigma	
PJB12-11																
27	70	78	0.89	0.1297	0.0008	6.6749	0.0623	0.3730	0.0030	2094	11	2069	8	2043	14	
28	98	95	1.03	0.1594	0.0011	10.0482	0.1935	0.4563	0.0082	2450	11	2439	18	2423	36	
30	45	46	0.98	0.1066	0.0011	4.5136	0.0589	0.3061	0.0023	1743	19	1734	11	1722	12	
31	44	36	1.22	0.1072	0.0011	4.4099	0.0531	0.2981	0.0025	1752	18	1714	10	1682	12	
32	175	65	2.70	0.1124	0.0013	5.0722	0.0668	0.3264	0.0018	1839	21	1832	11	1821	9	
33	198	152	1.30	0.2382	0.0013	20.2304	0.1694	0.6148	0.0041	3109	9	3102	8	3089	16	
34	106	119	0.89	0.1467	0.0008	8.7070	0.0558	0.4299	0.0021	2309	10	2308	6	2305	10	
35	223	160	1.40	0.1121	0.0009	5.0522	0.0399	0.3268	0.0016	1833	13	1828	7	1823	8	
36	33	23	1.41	0.1072	0.0010	4.4362	0.0734	0.2999	0.0045	1754	17	1719	14	1691	22	
37	94	109	0.86	0.1239	0.0011	6.1353	0.0630	0.3587	0.0022	2013	15	1995	9	1976	10	
38	91	67	1.35	0.1164	0.0010	5.4788	0.0569	0.3408	0.0020	1902	15	1897	9	1891	10	
40	34	41	0.83	0.1450	0.0013	8.1009	0.1794	0.4041	0.0074	2287	15	2242	20	2188	34	
41	106	177	0.60	0.1511	0.0008	9.1603	0.0845	0.4387	0.0028	2358	9	2354	8	2345	13	
42	148	135	1.09	0.1607	0.0011	10.3059	0.0953	0.4645	0.0025	2463	13	2463	9	2459	11	
43	69	105	0.66	0.1597	0.0013	10.1450	0.1043	0.4598	0.0027	2454	13	2448	10	2439	12	
44	93	108	0.86	0.1591	0.0012	9.8819	0.0883	0.4500	0.0030	2447	12	2424	8	2395	14	
46	35	39	0.90	0.1668	0.0015	10.6331	0.1157	0.4619	0.0033	2528	16	2492	10	2448	15	
47	44	26	1.71	0.1543	0.0016	9.4427	0.1304	0.4437	0.0045	2394	18	2382	13	2367	20	
48	101	99	1.02	0.1618	0.0019	10.4511	0.2871	0.4667	0.0085	2476	20	2476	26	2469	37	
49	98	95	1.03	0.1226	0.0018	6.1028	0.1083	0.3607	0.0033	1994	26	1991	16	1985	16	
51	74	91	0.81	0.1075	0.0019	4.5797	0.1343	0.3075	0.0059	1758	33	1746	24	1729	29	
53	128	87	1.47	0.1701	0.0054	11.3690	1.0457	0.4747	0.0308	2558	52	2554	86	2504	135	
54	153	150	1.02	0.1690	0.0024	11.2108	0.4001	0.4811	0.0170	2548	24	2541	33	2532	74	
55	99	90	1.10	0.1179	0.0019	5.5464	0.1144	0.3407	0.0040	1924	30	1908	18	1890	19	
56	99	72	1.37	0.1126	0.0021	4.8900	0.1192	0.3147	0.0047	1843	33	1801	21	1764	23	
57	78	74	1.04	0.1133	0.0019	5.2016	0.1143	0.3320	0.0043	1854	25	1853	19	1848	21	
58	175	128	1.37	0.1538	0.0007	9.2458	0.1510	0.4358	0.0070	2388	8	2363	15	2332	31	
59	83	63	1.31	0.1530	0.0014	9.2403	0.1402	0.4379	0.0057	2380	15	2362	14	2341	26	
60	50	52	0.96	0.1067	0.0012	4.5207	0.0954	0.3066	0.0053	1743	22	1735	18	1724	26	
61	77	126	0.61	0.1524	0.0026	9.3663	0.6560	0.4440	0.0270	2373	29	2375	64	2369	121	
63	91	103	0.88	0.1501	0.0011	8.8502	0.2574	0.4271	0.0117	2347	13	2323	27	2293	53	
64	24	10	2.41	0.1218	0.0062	5.4772	0.1647	0.3380	0.0098	1984	86	1897	26	1877	47	
65	208	116	1.79	0.1560	0.0009	9.6819	0.4641	0.4499	0.0223	2413	16	2405	44	2395	99	
66	97	138	0.71	0.1586	0.0010	9.8606	0.1583	0.4505	0.0068	2443	10	2422	15	2398	30	
67	38	135	0.28	0.1135	0.0016	5.1890	0.1357	0.3310	0.0072	1857	26	1851	22	1843	35	
68	33	38	0.87	0.1071	0.0012	4.5542	0.0581	0.3084	0.0022	1750	22	1741	11	1733	11	
69	87	132	0.65	0.1129	0.0013	4.9428	0.0622	0.3171	0.0018	1856	55	1810	11	1776	9	
70	16	193	0.09	0.1438	0.0013	7.9142	0.0831	0.3982	0.0021	2273	22	2221	10	2161	10	
71	32	37	0.88	0.1728	0.0031	11.5599	0.5171	0.4832	0.0173	2587	31	2569	42	2541	75	
72	145	64	2.25	0.1595	0.0022	10.1240	0.2546	0.4607	0.0141	2450	23	2446	23	2442	62	
73	226	121	1.87	0.1582	0.0017	10.0108	0.1674	0.4580	0.0057	2437	18	2436	15	2431	25	
74	112	88	1.28	0.1151	0.0011	5.3223	0.0743	0.3345	0.0033	1883	17	1873	12	1860	16	

Table 2. Cont.

No.	Conent (ppm)			Th/U	Isotopic Ratios						Age (Ma)					
	Th	U			$^{207}\text{Pb}/^{206}\text{Pb}$	1 Sigma	$^{207}\text{Pb}/^{235}\text{U}$	1 Sigma	$^{206}\text{Pb}/^{238}\text{U}$	1 Sigma	$^{207}\text{Pb}/^{206}\text{Pb}$	1 Sigma	$^{207}\text{Pb}/^{235}\text{U}$	1 Sigma	$^{206}\text{Pb}/^{238}\text{U}$	1 Sigma
PJB12-11																
75	95	85	1.12	0.2280	0.0015	18.7653	0.2371	0.5962	0.0068	3038	11	3030	12	3015	28	
76	94	47	2.02	0.1579	0.0012	9.7923	0.1422	0.4488	0.0054	2435	13	2415	13	2390	24	
77	169	241	0.70	0.1538	0.0009	9.4554	0.1502	0.4452	0.0066	2389	5	2383	15	2374	29	
78	26	18	1.44	0.1080	0.0011	4.3605	0.0899	0.2929	0.0057	1766	19	1705	17	1656	29	
79	152	139	1.10	0.1123	0.0011	5.0301	0.0656	0.3252	0.0038	1836	17	1824	11	1815	18	
80	33	39	0.85	0.1068	0.0008	4.5407	0.0540	0.3085	0.0034	1746	14	1739	10	1733	17	
81	27	22	1.24	0.1078	0.0008	4.6187	0.0897	0.3104	0.0057	1763	13	1753	16	1743	28	
82	49	57	0.87	0.1124	0.0011	4.7773	0.0710	0.3076	0.0030	1839	19	1781	13	1729	15	
83	98	61	1.61	0.1068	0.0008	4.5527	0.0426	0.3093	0.0024	1746	14	1741	8	1738	12	
84	115	165	0.70	0.1607	0.0010	10.2960	0.1003	0.4640	0.0033	2465	10	2462	9	2457	15	
85	56	58	0.97	0.1131	0.0014	5.0517	0.0749	0.3231	0.0018	1850	22	1828	13	1805	9	
86	87	53	1.64	0.1260	0.0010	6.3753	0.0621	0.3668	0.0024	2043	14	2029	9	2014	11	
87	90	224	0.40	0.1126	0.0011	5.1336	0.0586	0.3305	0.0021	1843	13	1842	10	1841	10	
88	128	117	1.09	0.1686	0.0020	11.1488	0.1921	0.4779	0.0039	2544	20	2536	16	2518	17	
89	108	108	1.00	0.1629	0.0019	10.5746	0.1816	0.4694	0.0040	2487	20	2487	16	2481	18	
90	41	57	0.71	0.1142	0.0012	5.2394	0.0614	0.3328	0.0021	1933	17	1859	10	1852	10	
92	73	85	0.86	0.1700	0.0010	11.4092	0.0855	0.4867	0.0027	2558	10	2557	7	2557	12	
93	57	79	0.73	0.1704	0.0010	11.3359	0.0965	0.4821	0.0031	2561	10	2551	8	2537	14	
94	79	63	1.25	0.1698	0.0027	11.3223	0.2297	0.4833	0.0067	2555	27	2550	19	2542	29	
95	6	82	0.07	0.0884	0.0012	2.8745	0.0878	0.2338	0.0057	1391	26	1375	23	1355	30	
96	29	28	1.07	0.1073	0.0011	4.5792	0.0603	0.3093	0.0028	1754	18	1746	11	1737	14	
97	110	111	0.99	0.1473	0.0009	7.2872	0.0812	0.3585	0.0038	2315	10	2147	10	1975	18	
98	48	42	1.16	0.1359	0.0013	7.3201	0.0776	0.3903	0.0024	2176	17	2151	10	2124	11	
99	43	39	1.11	0.1777	0.0015	12.2345	0.1285	0.4984	0.0033	2631	19	2623	10	2607	14	
100	88	48	1.81	0.1688	0.0023	10.7511	0.2861	0.4608	0.0078	2545	24	2502	25	2443	35	



**Figure 4.** Representative zircon grain cathodoluminescence (CL) images with  $^{207}\text{Pb}/^{206}\text{Pb}$  ages, and  $\epsilon\text{Hf}(t)$  values (within parentheses). The analysis positions are shown, with solid lines for  $^{207}\text{Pb}/^{206}\text{Pb}$  ages and dashed lines for Hf isotope values.



**Figure 5.** Th/U values of zircon grains with  $^{207}\text{Pb}/^{206}\text{Pb}$  ages.

#### 4.1. Sample JJZ12-08

The zircon grains collected from sample JJZ12-08 were mostly well rounded to short columnar in shape, with grain sizes ranging from 100  $\mu\text{m}$  to 500  $\mu\text{m}$  (Figure 4). One hundred zircon grain U-Pb ages were obtained, and 6 more discordant ( $>5\%$ ) zircon grains were discarded. Uranium concentrations ranged from 8 to 220 ppm, and thorium from 5 to 561 ppm. The Th/U values are mostly greater than 0.4 and are clustered at 0.6 to 1.5 (Figure 5), which, combined with the oscillatory growth zoning in CL images, indicates their magmatic origin [62–65]. The 94 grains yield three age populations: 1739–1799 Ma, with a weighted average age of  $1774 \pm 8$  Ma ( $n = 22$ , MSWD = 0.73); 1839–1857 Ma, with a weighted average age of  $1849 \pm 8$  Ma ( $n = 22$ , MSWD = 0.08); and 2436–2465 Ma with a weighted average age of  $2453 \pm 8$  Ma ( $n = 10$ , MSWD = 0.71) (Figures 6 and 7). There are two smaller populations with ages in the ranges of 1872–1907 Ma and 1945–2000 Ma, and a few ages are plotted in the ranges 2068–2394 Ma and 2526–2611 Ma. Four younger magmatic detrital zircon ages are obtained; the youngest is  $1657 \pm 17$  Ma (JJZ12-08-2).

Lu-Hf isotopic analyses were performed on the 94 grains already used for zircon U-Pb age dating.  $\varepsilon\text{Hf}(t)$  values from these zircon grains cluster into two main populations of  $-1$  to  $-8$  and  $+1$  to  $+8$ , corresponding to age ranges of 1.7–1.9 Ga and 2.3–2.6 Ga, respectively (Figure 8). The zircon population with an age of 1739–1799 Ma has one zircon grain with a positive  $\varepsilon\text{Hf}(t)$  value of 2.38, whereas the other grains have negative  $\varepsilon\text{Hf}(t)$  values from  $-0.08$  to  $-9.20$ ,  $^{176}\text{Hf}/^{177}\text{Hf}$  values of 0.281420 to 0.281678, and two-stage Hf model ages ( $T_{\text{DM2}}$ ) of 2429–2993 Ma. The zircon population with age of 1839–1857 Ma has five zircon grains with positive  $\varepsilon\text{Hf}(t)$  values of 0.80 to 5.08, whereas the other grains have negative  $\varepsilon\text{Hf}(t)$  values from  $-1.20$  to  $-8.07$ ,  $^{176}\text{Hf}/^{177}\text{Hf}$  values of 0.281409 to 0.281605, and  $T_{\text{DM2}}$  of 2579–2998 Ma. The zircon population with an age of 2436–2465 Ma has one zircon grain with a high positive  $\varepsilon\text{Hf}(t)$  value of 14.05, whereas the other grains have positive  $\varepsilon\text{Hf}(t)$  values from 1.11 to 5.13,  $^{176}\text{Hf}/^{177}\text{Hf}$  values of 0.281288 to 0.281432, and  $T_{\text{DM2}}$  of 2657–2894 Ma.

#### 4.2. Sample PJB12-11

The zircon grains collected from sample PJB12-11 were mostly well rounded to short columnar in shape, with grain sizes ranging from 100  $\mu\text{m}$  to 500  $\mu\text{m}$  (Figure 4). One hundred zircon grain U-Pb ages were obtained and eight more discordant zircon grains were ignored. Uranium concentrations range from 10 to 510 ppm, and thorium from 6 to 374 ppm. The Th/U values are mostly greater than 0.4 and are clustered at 0.6 to 1.5 (Figure 5), which, combined with the oscillatory growth zoning in the CL images, indicates their magmatic origin [62–65]. The 92 grains yield three age populations: 1743–1766 Ma, with a weighted average age of  $1752 \pm 9$  Ma ( $n = 14$ , MSWD = 0.17); 1831–1863 Ma, with a weighted average age of  $1844 \pm 11$  Ma ( $n = 13$ , MSWD = 0.28); and 2435–2476 Ma with a weighted average age of  $2449 \pm 6$  Ma ( $n = 15$ , MSWD = 0.70) (Figures 6 and 7). In addition, there are two smaller population ages:  $2381 \pm 6$  Ma ( $n = 11$ , MSWD = 1.8, ranging from 2347–2394 Ma) and  $2551 \pm 10$  Ma ( $n = 10$ , MSWD = 0.50, ranging from 2528–2561 Ma). Furthermore, there are a few ages which are plotted between 1883–2315 Ma. There are also two older ages (3038 Ma and 3109 Ma), and one younger metamorphic age (1391 Ma with the Th/U value of 0.07).

Lu-Hf isotopic analyses were performed on the 92 samples already used for zircon U-Pb age dating.  $\varepsilon\text{Hf}(t)$  values from these zircon grains cluster into two main populations of  $-0.5$  to  $-9$  and  $1$  to  $8$ , corresponding to age ranges of 1.7 Ga to 1.9 Ga and 2.3 Ga to 2.6 Ga, similar to sample JZZ12-08 (Figure 8). The zircon grain population with an age range of 1743–1766 Ma has zircon grains with negative  $\varepsilon\text{Hf}(t)$  values from  $-4.46$  to  $-11.16$ ,  $^{176}\text{Hf}/^{177}\text{Hf}$  values of 0.281367 to 0.281566, and two-stage Hf model ages ( $T_{\text{DM2}}$ ) of 2694–3113 Ma. The zircon grain population with an age of 1831–1863 Ma has zircon grains with negative  $\varepsilon\text{Hf}(t)$  values from  $-0.52$  to  $-9.37$ ,  $^{176}\text{Hf}/^{177}\text{Hf}$  values of 0.281364 to 0.281627, and two-stage Hf model ages ( $T_{\text{DM2}}$ ) of 2536–3072 Ma. The zircon population with an age of 2435–2476 Ma has two zircon grains with negative  $\varepsilon\text{Hf}(t)$  values of  $-8.92$  and  $-4.28$ , whereas the other grains have  $\varepsilon\text{Hf}(t)$  values from 0.23 to 5.24, with  $^{176}\text{Hf}/^{177}\text{Hf}$  values of 0.281247 to 0.281388 and  $T_{\text{DM2}}$  of 2638–2951 Ma.

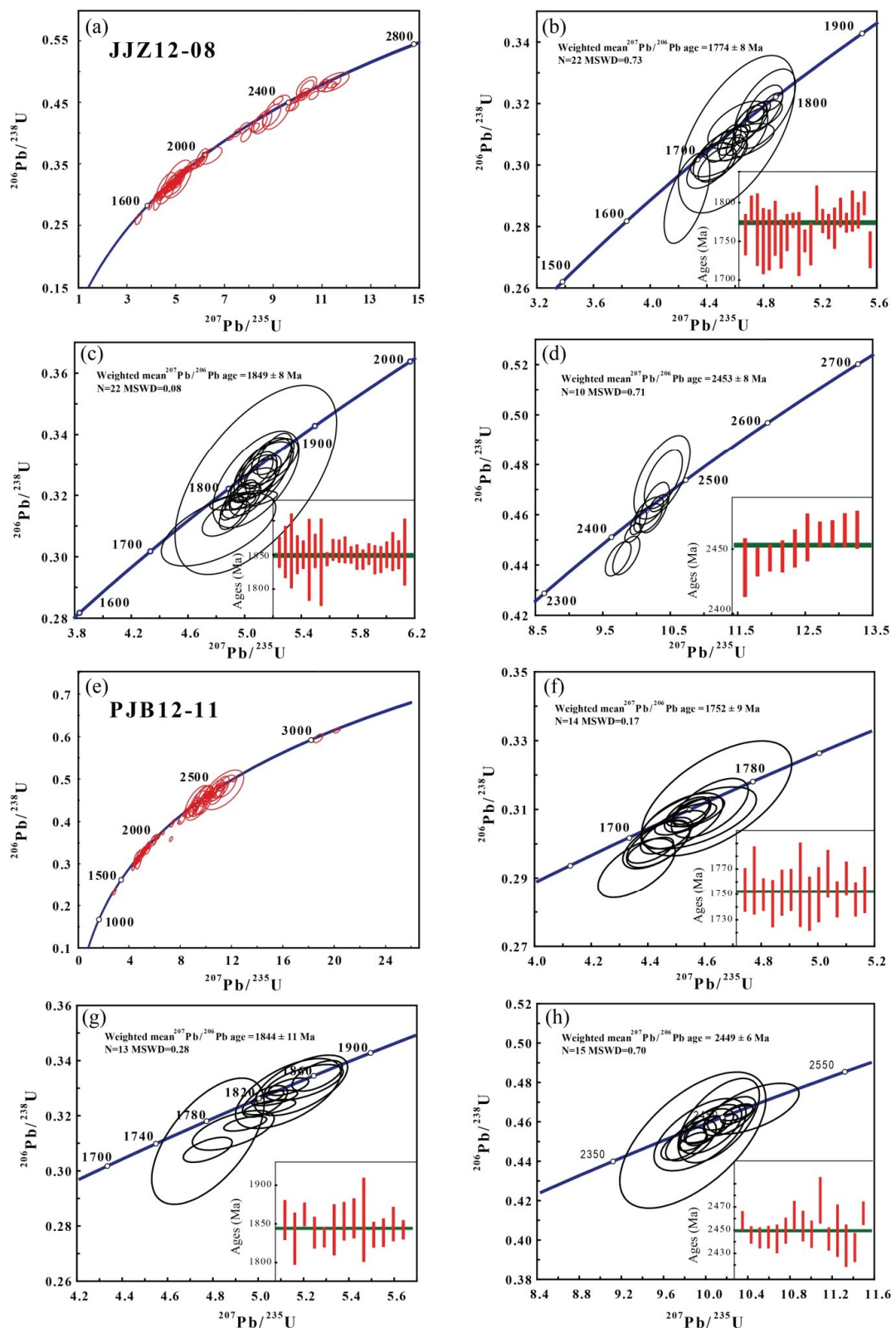


**Figure 6.** U-Pb concordia and peak age distribution diagrams of zircon grains from samples JJZ12-08 (a-d) and PJB12-11 (e-h) collected from the Chuanlinggou Formation.

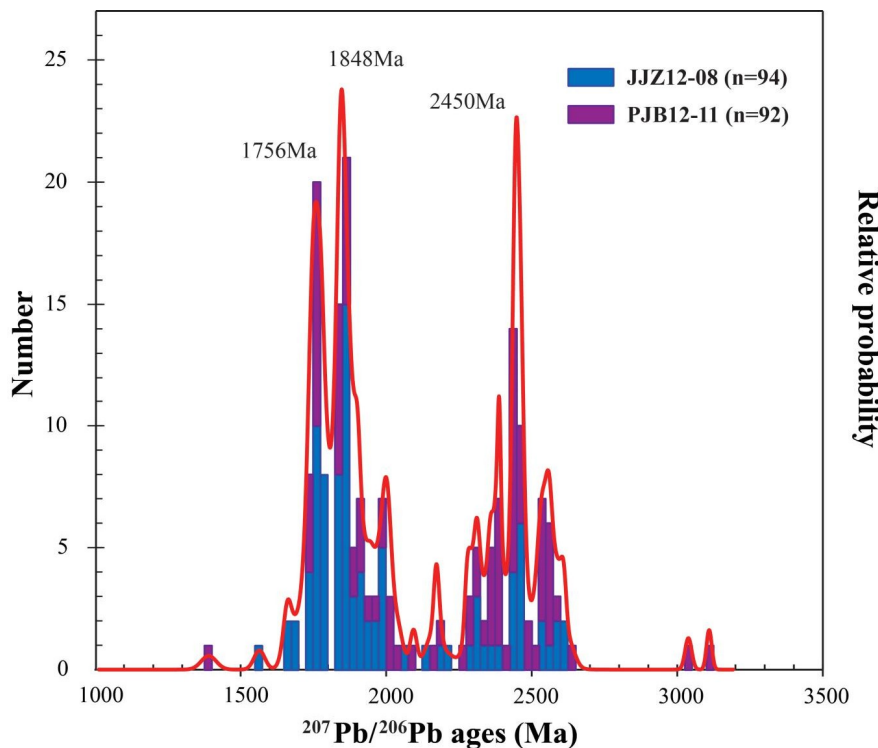


**Figure 7.** Relative probability of the detrital zircon grains' U-Pb ages.

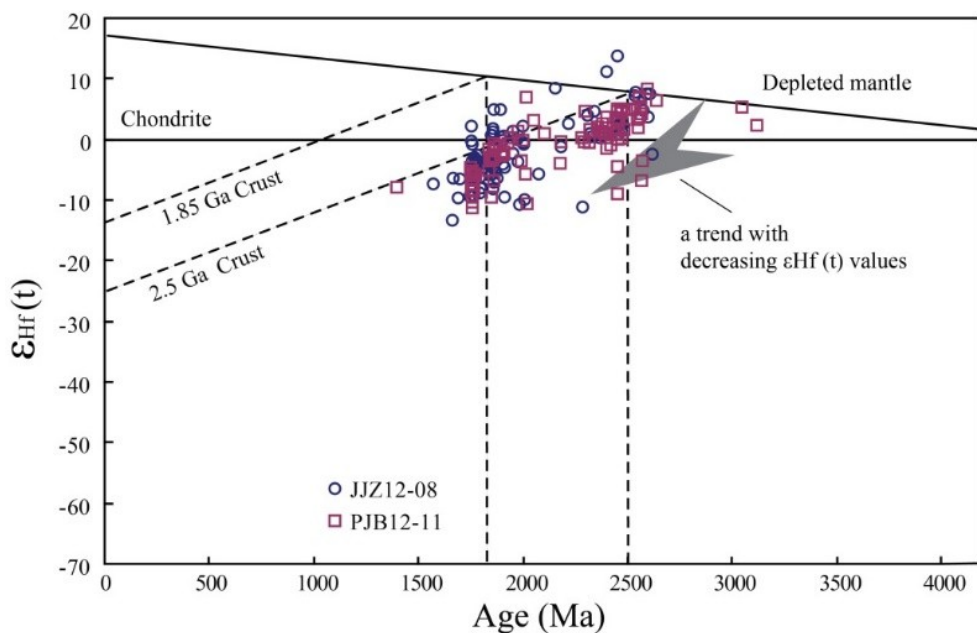


**Figure 8.**  $\epsilon\text{Hf}(t)$  values versus U-Pb ages of detrital zircon grains from JJZ12-08 and PJB12-11. The dashed lines indicate the evolution trends of average continental crust ( $^{176}\text{Lu}/^{177}\text{Hf} = 0.015$ ).

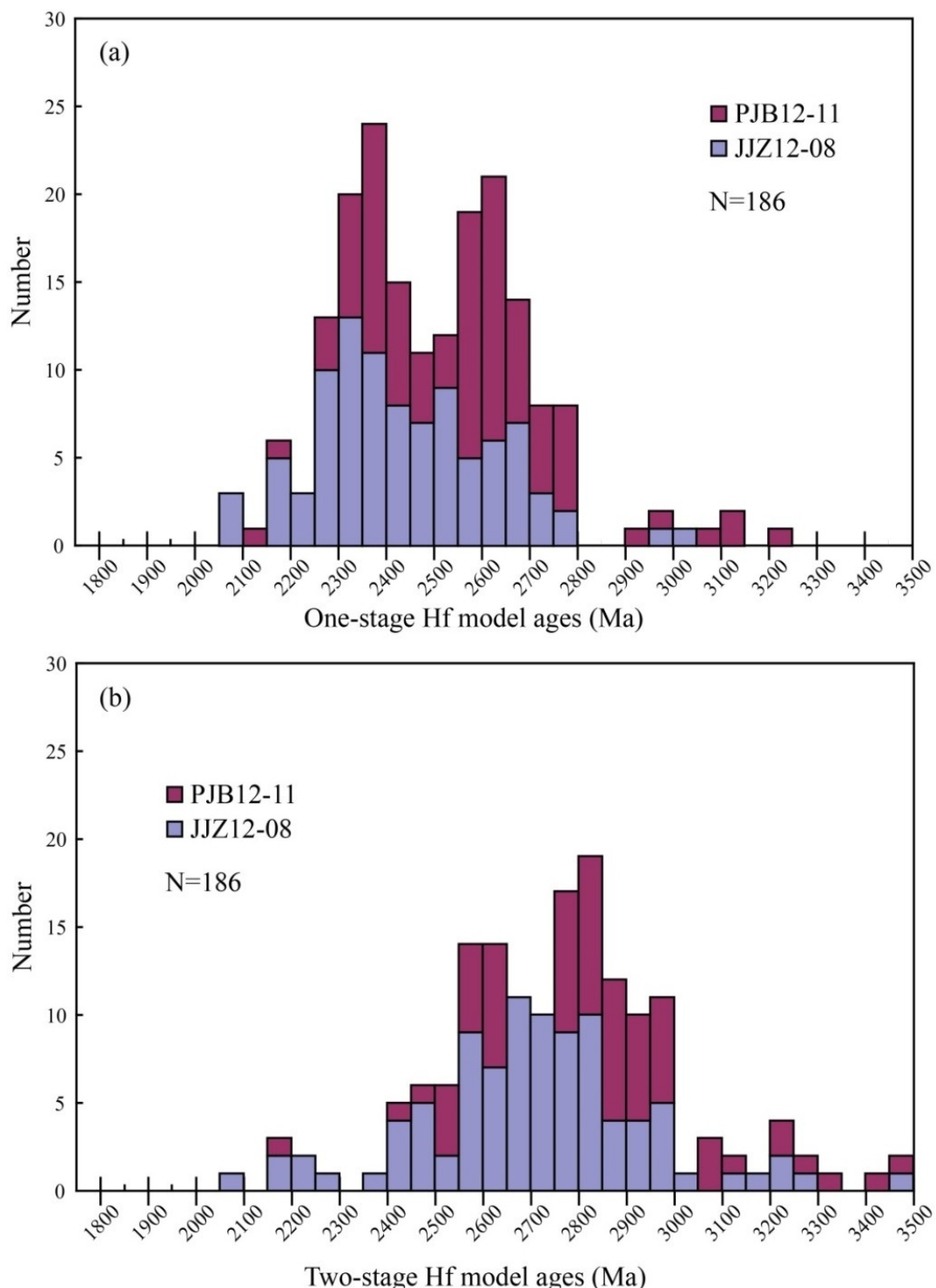


**Figure 9.** (a) Histogram of the one-stage Hf model ages of detrital zircon grains from JJZ12-08 and PJB12-11; (b) Histogram of the two-stage Hf model ages of detrital zircon grains from JJZ12-08 and PJB12-11.

## 5. Discussion

### 5.1. Geochronology of the Sedimentary Iron Deposit

During the Mesoproterozoic, the North China Craton underwent a long period of sedimentation. In the geological time scale of China (GTSC), the lower to upper Mesoproterozoic consists of the

Changchengian and Jixianian systems. Within the older Changchengian System, the lowermost Changzhougou and Chuanlinggou Formations (Figure 2) unconformably overlie the Archean to Paleoproterozoic crystalline basement sequence. Gao et al. (2009) [66] obtained an emplacement age of  $1638 \pm 14$  Ma by SHRIMP U-Pb dating method for a diabase dike crosscutting the Chuanlinggou Formation at Jixian. Zhang et al. (2013) [67] obtained an emplacement age of  $1634 \pm 9$  Ma by LA-ICP-MS U-Pb dating method for a dioritic porphyrite dyke emplaced into the Chuanlinggou Formation at Jixian. Sun et al. (2013) [68] obtained an age for the tuff from the upper most part of the Chuanlinggou Formation of  $1621 \pm 12$  Ma by SHRIMP U-Pb dating method, which is within the error range of the intrusion ages in this formation. These geochronological ages constrain the Chuanlinggou Formation deposition age to be not later than 1638 Ma. He et al. (2011) [69] obtained paleo-weathered mantle clastic rock detrital zircon U-Pb ages of  $1682 \pm 20$  Ma and  $1708 \pm 6$  Ma by SHRIMP and LA-ICP-MS dating methods. These rocks are covered directly by the sandstones of the Changzhougou Formation, suggesting that the age of the base of the Changzhougou Formation should be younger than 1682 Ma. Li et al. (2011, 2013) [70,71] obtained granite-porphyry dike ages of  $1673 \pm 10$  Ma and  $1669 \pm 20$  Ma by LA-MC-ICP-MS and SHRIMP U-Pb dating methods, and these dykes are unconformably overlain by the conglomerates and sandstones of the Changzhougou Formation, further suggesting that the base age of the Changchengian System in the NCC should be younger than 1670 Ma. This also implies that the Chuanlinggou Formation deposition age is not older than 1670 Ma.

In this study, a total of 186 U-Pb analyses of detrital zircon grains from two samples of the Chuanlinggou Formation in the Xuanhua area yield apparent  $^{207}\text{Pb}/^{206}\text{Pb}$  ages (Th/U value > 0.4) ranging from 1657–3109 Ma. The two samples display similar age population ranges. The detrital zircon age spectra can be broadly subdivided into three major age populations: 1.74–1.8 Ga, with a peak age of 1765 Ma; 1.84–1.86 Ga, with a peak age of 1848 Ma; and 2.44–2.48 Ga, with a peak age of 2450 Ma (Figure 7). There is a distinctly young age in each of the two samples: 1565 Ma (JJZ12-08-14) and 1391 Ma (PJB12-11-95) with Th/U values of 0.24 and 0.07, respectively, and the reason for these clear outlier ages is uncertain. Minimum depositional ages are interpreted from populations of multiple grains. There are four zircon grain U-Pb ages in the youngest zircon age group (JJZ12-08-2,  $1657 \pm 17$  Ma; JJZ12-08-1,  $1661 \pm 12$  Ma; JJZ12-08-84,  $1683 \pm 20$  Ma; and JJZ12-08-17,  $1694 \pm 30$  Ma), with high Th/U values (0.75–1.49) and oscillatory zoning. Conventionally, the maximum depositional age of the sediments can be constrained by the age of the youngest zircon grains, which has not been altered since deposition. Therefore, the zircon U-Pb age constrains the depositional age of the Xuanlong type iron deposit to be not older than 1657 Ma. Combining this information with previous studies, and considering the considerable thickness of this formation, this type of iron deposit was deposited at 1634–1657 Ma, close to 1650 Ma.

## 5.2. Crustal Growth and Evolution of the Trans-North China Orogen

### 5.2.1. Evolution of the Trans-North China Orogen

The North China Craton has experienced a long geological evolutionary history (ca. 3.8 Ga) [1–3,72–76]. Its central segment, the TNCO, is most significant, as it is a result of the collision between the Eastern and Western blocks, and preserves important clues for revealing the tectonic evolution history of the NCC. Zhao et al. (2005, 2012) [2,7] and Lu et al. (2008) [9] reviewed the geochronological data of nearly all metamorphic complexes (Chengde, Xuanhua, Huai'an, Hengshan, Wutai, Fuping, Zanhuang, Lvliang, and Taihua) in this area, and discovered that the age of the final amalgamation of the NCC was ~1.85 Ga. Recently, Tang and Santosh (2018) [77] summarized the geology, geochemical, and geochronology data of the Neoarchean to Paleoproterozoic rocks from the TNCO. They attempted to reconstruct the major Precambrian events of the NCC, which experienced amalgamation (Ordos, Qianhuai and Xuchang microblocks; 2.58–2.48 Ga, leading to the initial cratonisation of the NCC), post-collisional extension (2.50–2.45 Ga), subduction (which occurred in the Hengshan, Huai'an-Xuanhua and Lvliang Complexes),

rifting (which occurred in the Fuping, Wutai and Zanhuang Complexes, and slightly later in the Hengshan, Huai'an-Xuanhua, and Zanhuang Complexes; 2.45–1.98 Ga), the assembly of the separated terranes (or complexes) driven by the amalgamation of the Western and Eastern blocks (1.96–1.80 Ga), and finally, the termination of the collisional event (1.80–1.74 Ga). It is recognized that the NCC is one part of the Columbia Supercontinent [7,18,78–82]. During the period of 1.85–1.7 Ga, the NCC was evolved in an extensional tectonic regime [16,44], with extension and uplift in the interior and at the edge of the craton. This led to the intrusion of Mg-rich mafic dykes, plagioclases, gabbros, mangerites, rapakivi granites, A-type granite, and potassium-rich volcanic rocks, corresponding to late Paleoproterozoic to early Mesoproterozoic global non-orogenic magmatic activity during the breakup of the Columbia supercontinent [4,6,22,45,78,83–94]. The dyke swarms represent the initial breakup of the supercontinent [81]. Lu et al. (2008) [9] reviewed the geochronology data of the intrusive and volcanic rocks and suggested that during the period 1.8–1.6 Ga, the extensional tectonic events of the NCC could be divided into three peak stages (at 1.78 Ga, 1.70 Ga, and 1.62 Ga).

Detrital zircon ages from the Chuanlinggou Formation contain zircon populations defining peaks similar to the two major events at 1848 Ma and 2450 Ma, which align with the ages mentioned above. These two major tectonic-thermal event ages (ca. 1.85 Ga and ca. 2.5 Ga) have been widely recognized [7,16,19–21,24,93,95–99]. However, there is still debate surrounding the processes of the crustal amalgamation and cratonisation. In this work, another age population of 1.74–1.80 Ga from the Chuanlinggou Formation has been discovered. This is consistent with the age of the mafic dyke swarms which must have caused crustal melting, which recorded the extension, uplift, crust–mantle interaction and mantle upwelling events after 1.8 Ga in the central part of the NCC.

### 5.2.2. Crustal Growth

Detrital zircon U-Pb age spectra coupled with Hf isotope data can be used to provide insight into crustal growth and recycling, as well as provenance [100–103]. Hf isotope data from the Chuanlinggou Formation show two obvious groups, with different  $\epsilon\text{Hf}$  ( $t$ ) values. Most of the detrital zircon grains with U-Pb age ranges of 1.7–1.9 Ga have modest negative  $\epsilon\text{Hf}$  ( $t$ ) values, clustering at –1 to –8, suggesting that the source rocks of these zircon grains were derived from the recycling of somewhat more ancient crust. Most of the detrital zircons with age ranges of 2.3–2.6 Ga have  $\epsilon\text{Hf}$  ( $t$ ) values, clustering at +1 to +8. However, these older zircon grains' Hf two-stage model ages do not show the expected ca. 2.5 Ga peak, but instead indicate a peak at 2.6–2.9 Ga, which is slightly older than the apparent age and single stage Hf model peak age (Figure 9), suggesting that the rocks were not directly derived from the differentiation of the depleted mantle; i.e., from basalt. The source rocks of these zircon grains might be derived from juvenile crust with a short period of reworking while residing in the crust [104]. It is obvious that there is a trend of decreasing  $\epsilon\text{Hf}$  ( $t$ ) values with ages (Figure 8), which also suggests that, within this period, the younger zircon grains are being derived from greater amounts of reworking of an older crust, or the reworking of recently formed crust; i.e., 2.6 Ga crust has been reworked to form 2.3 Ga crust. In addition, the two ancient grains found hint at the presence of truly ancient crust in this reworking period. These features are earmarks of the crustal evolution of the North China Craton and are consistent with previous studies in the TNCO (Zhang et al., 2013 [105] and references therein) and similar to those in the East Block and West Block [104,106–112]. Furthermore, detrital zircon grains from all of these studies have a similar two-stage Hf model age ( $T_{\text{DM2}}$ ) ranges of 2.4–3.0 Ga, with a peak age of 2.65–2.85 Ga, implying the possibility of crust–mantle differentiation during this period, marking the most significant stage of crustal growth of the NCC. This is similar to the Nd model age peak at 2.8–2.4 Ga obtained by Wu et al. (2005) [113].

## 6. Conclusions

The following are the conclusions of this study.

- (1) Three zircon grain population age ranges within the Chuanlinggou Formation have been observed, with peak ages of 2450 Ma, 1848 Ma, and 1765 Ma, representing periods of magmatism associated with the amalgamation and breaking up events of the NCC;
- (2) Combined with previous studies, the sedimentary type of iron deposit hosted by the Chuanlinggou Formation was formed at 1634–1657 Ma, close to 1650 Ma;
- (3) Detrital zircon grains from the Chuanlinggou Formation form two obvious groups, with different  $\epsilon_{\text{Hf}}(t)$  values ranging from −1 to −8 and from 1 to 8, which correspond to the age ranges of 1.7–1.9 Ga and 2.3–2.6 Ga, respectively. They have a similar two-stage Hf model age peak at 2.65–2.85 Ga, suggesting that the source rocks were derived from the recycling of ancient crusts. It also implies the possibility of crust–mantle differentiation during this period, marking the most significant stage of crustal growth of the NCC.

**Author Contributions:** Y.L. (Yanhe Li) and C.D. conceived this contribution. C.D., Y.L. (Yanhe Li), Y.Y., Y.L. (Yongsheng Liang) and M.W. made field investigation. C.D. performed the zircon U-Pb dating and Lu-Hf isotope analysis. C.D., Y.L. (Yanhe Li) and K.H. interpreted all the data. C.D. wrote the original draft of the paper. Y.L. (Yanhe Li) reviewed the original draft of paper.

**Funding:** This work was jointly funded by the National Natural Science Foundation of China (No. 41402078 and 41473014), National Basic Research Program of China (973 Program) (2012CB416801), and a Grant of the Chinese Ministry of Land and Resources Public Benefit Research Foundation of China (No. 201211074).

**Acknowledgments:** We gratefully thank Chunli Guo and Qian Wang from the Institute of Mineral Resources, Chinese Academy of Geological Sciences for their important guidance and assistance in zircon age testing, Hf isotope testing, and data analysis. We would like thank two anonymous reviewers for their helpful comments and insightful reviews, which have greatly improved the manuscript.

**Conflicts of Interest:** The authors declare no conflict of interest.

## References

1. Zhao, G.-C.; Wilde, S.A.; Cawood, P.A.; Sun, M. Archean blocks and their boundaries in the North China Craton: Lithological, geochemical, structural and P-T path constraints and tectonic evolution. *Precambrian Res.* **2001**, *107*, 45–73. [[CrossRef](#)]
2. Zhao, G.-C.; Sun, M.; Wilde, S.A.; Li, S.-Z. Late Archean to Paleoproterozoic evolution of the North China Craton: Key issues revisited. *Precambrian Res.* **2005**, *136*, 177–202. [[CrossRef](#)]
3. Zhai, M.-G.; Santosh, M. The early Precambrian odyssey of North China craton: A synoptic overview. *Gondwana Res.* **2011**, *20*, 6–25. [[CrossRef](#)]
4. Zhai, M.-G. 2.1–1.7 Ga geological event group and its geotectonic significance. *Acta Petrol. Sin.* **2004**, *20*, 1343–1354, (In Chinese with English abstract).
5. Zhai, M.-G. Lower crust and lithospheric mantle beneath the North China Craton before the Mesozoic lithospheric disruption. *Acta Petrol. Sin.* **2008**, *24*, 2185–2204. (In Chinese with English abstract)
6. Zhai, M.-G. Evolution of the North China Craton and early plate tectonics. *Acta Geol. Sin.* **2012**, *86*, 1135–1149. (In Chinese with English abstract)
7. Zhao, G.-C.; Cawood, P.A.; Li, S.-Z.; Wilde, S.A.; Sun, M.; Zhang, J.; He, Y.-H.; Yin, C.-Q. Amalgamation of the North China Craton: Key issues and discussion. *Precambrian Res.* **2012**, *222–223*, 55–76. [[CrossRef](#)]
8. Wu, C.-H. Meta-Sedimentary Rocks and Tectonic Division of the North China Craton. *Geol. J. China Univ.* **2007**, *13*, 442–457. (In Chinese with English abstract)
9. Lu, S.-N.; Zhao, G.-C.; Wang, H.-M.; Hao, G.-J. Precambrian metamorphic basement and sedimentary cover of the North China Craton: A review. *Precambrian Res.* **2008**, *160*, 77–93. [[CrossRef](#)]
10. Zheng, Y.-F.; Wu, F.-Y. Growth and reworking of cratonic lithosphere. *Chin. Sci. Bull.* **2009**, *54*, 3347–3353. [[CrossRef](#)]
11. Zhu, R.-X.; Zheng, T.-Y. Destruction geodynamics of the North China Craton and its Paleoproterozoic plate tectonics. *Chin. Sci. Bull.* **2009**, *54*, 3354–3366. [[CrossRef](#)]
12. Wang, H.-C.; Yu, H.-F.; Miao, P.-S.; Zhao, F.-Q.; Xiang, Z.-Q. Precambrian Research in China: New Advances and Perspectives. *Geol. Surv. Res.* **2011**, *34*, 241–253. (In Chinese with English abstract)

13. Bai, J.; Huang, X.-G.; Dai, F.-Y.; Wu, C.-H. *The Precambrian Evolution of China*; Geological Publishing House: Beijing, China, 1993; pp. 65–79. (In Chinese)
14. Wu, J.-S.; Geng, Y.-S.; Shen, Q.-H.; Wang, Y.-S.; Liu, D.-Y.; Song, B. *Archean Geology Characteristics and Tectonic Evolution of Sino-Korea Paleo-Continent*; Geological Publishing House: Beijing, China, 1998; pp. 1–104. (In Chinese)
15. Zhai, M.-G.; Bian, A.-G.; Zhao, T.-P. Amalgamation of the supercontinental of the North China Craton and its break up during late-middle Proterozoic. *Sci. China* **2000**, *43*, 219–232. [[CrossRef](#)]
16. Zhai, M.-G.; Peng, P. Paleoproterozoic events in the North China Craton. *Acta Petrol. Sin.* **2007**, *23*, 2665–2682. (In Chinese with English abstract)
17. Zhai, M.-G. Tectonic evolution and metallogenesis of North China Craton. *Miner. Depos.* **2010**, *29*, 24–36. (In Chinese with English abstract)
18. Wilde, S.A.; Zhao, G.-C.; Sun, M. Development of the North China Craton during the late Archaean and its final amalgamation at 1.8 Ga: Some speculations on its position within a global Paleoproterozoic supercontinent. *Gondwana Res.* **2002**, *5*, 85–94. [[CrossRef](#)]
19. Wilde, S.A.; Zhao, G.-C. Late Archean to Paleoproterozoic evolution of the North China Craton. *J. Asian Earth Sci.* **2005**, *24*, 519–522. [[CrossRef](#)]
20. Kröner, A.; Wilde, S.A.; Li, J.-H.; Wang, K.-Y. Age and evolution of a late Archean to early Palaeozoic upper to lower crustal section in the Wutaishan/Hengshan/Fuping terrain of northern China. *J. Asian Earth Sci.* **2005**, *24*, 577–595. [[CrossRef](#)]
21. Kröner, A.; Wilde, S.A.; O'Brien, P.J.; Li, J.-H.; Passchier, C.W.; Walte, N.P.; Liu, D.-Y. Field relationships, geochemistry, zircon ages and evolution of a late Archean to Paleoproterozoic lower crustal section in the Hengshan Terrain of Northern China. *Acta Geol. Sin.* **2005**, *79*, 605–629.
22. Kröner, A.; Wilde, S.A.; Zhao, G.-C.; O'Brien, P.J.; Sun, M.; Liu, D.-Y.; Wan, Y.-S.; Liu, S.-W.; Guo, J.-H. Zircon geochronology of mafic dykes in the Hengshan Complex of northern China: Evidence for late Paleoproterozoic rifting and subsequent high-pressure event in the North China Craton. *Precambrian Res.* **2006**, *146*, 45–67.
23. Zhang, S.-H.; Liu, S.-W.; Zhao, Y.; Yang, J.-H.; Song, B.; Liu, X.-M. The 1.75–1.68 Ga anorthosite-mangerite-alkali granitoid-rapakivi granite suite from the northern North China Craton: Magmatism related to a Paleoproterozoic orogen. *Precambrian Res.* **2007**, *155*, 287–312. [[CrossRef](#)]
24. Liu, C.-H.; Liu, F.-L.; Zhao, G.-C. The Paleoproterozoic basin evolution in the Trans-North China Orogen, North China Craton. *Acta Petrol. Sin.* **2012**, *28*, 2770–2784. (In Chinese with English abstract)
25. Kusky, T.M.; Li, J.-H. Paleoproterozoic tectonic evolution of the North China Craton. *J. Asian Earth Sci.* **2003**, *22*, 383–397. [[CrossRef](#)]
26. Kusky, T.M. Geophysical and geological tests of tectonic models of the North China Craton. *Gondwana Res.* **2011**, *20*, 26–35. [[CrossRef](#)]
27. Li, J.-H.; Kusky, T.M. A Late Archean foreland fold and thrust belt in the North China Craton: Implications for early collisional tectonics. *Gondwana Res.* **2007**, *12*, 47–66. [[CrossRef](#)]
28. Polat, A.; Herzberg, C.; Münker, C.; Rodgers, R.; Kusky, T.; Li, J.-H.; Fryer, B.; Dalaney, J. Geochemical and petrological evidence for a suprasubduction zone origin of Neoarchean (ca. 2.5 Ga) peridotites, central orogenic belt, North China craton. *Geol. Soc. Am. Bull.* **2006**, *118*, 771–784. [[CrossRef](#)]
29. Shen, B.-F.; Zhai, A.-M.; Chen, W.-L.; Yang, C.-L. *The Precambrian Mineralization of China*; Geology Publishing House: Beijing, China, 2006. (In Chinese)
30. Zhai, M.-G.; Santosh, M. Metallogeny of the North China Craton: Link with secular changes in the evolving Earth. *Gondwana Res.* **2013**, *24*, 275–297. [[CrossRef](#)]
31. Li, Y.-H.; Hou, K.-J.; Wan, D.-F.; Zhang, Z.-J. A compare geochemistry study for Algoma-and Superior-type banded iron formations. *Acta Petrol. Sin.* **2012**, *28*, 3513–3519. (In Chinese with English abstract)
32. Li, Y.-H.; Hou, K.-J.; Wan, D.-F.; Zhang, Z.-J.; Yue, G.-L. Precambrian banded iron formations in the North China Craton: Silicon and oxygen isotopes and genetic implications. *Ore Geol. Rev.* **2014**, *57*, 299–307. [[CrossRef](#)]
33. Li, H.-M.; Chen, Y.-C.; Li, L.-X.; Wang, D.-H. *Mineralization Regularity of Iron Deposits in China*; Geology Publishing House: Beijing, China, 2012; pp. 1–246. (In Chinese)

34. Wan, Y.-S.; Dong, C.-Y.; Xie, H.-Q.; Wang, S.-J.; Song, C.-M.; Xu, Z.-Y.; Wang, S.-Y.; Zhou, H.-Y.; Ma, M.-Z.; Liu, D.-Y. Formation ages of early Precambrian BIFs in the North China Craton: SHRIMP zircon U-Pb dating. *Acta Geol. Sin.* **2012**, *86*, 1447–1478. (In Chinese with English abstract)
35. Zhang, L.-C.; Zhai, M.-G.; Wan, Y.-S.; Guo, J.-H.; Dai, Y.-P.; Wang, C.-L.; Liu, L. Study of the Precambrian BIF-iron deposits in the North China Craton: Progresses and questions. *Acta Petrol. Sin.* **2012**, *28*, 3431–3445. (In Chinese with English abstract)
36. Shen, B.-F. Geological characters and resource prospect of the BIF type iron ore deposits in China. *Acta Geol. Sin.* **2012**, *86*, 1377–1396. (In Chinese with English abstract)
37. Zhao, Y.-M. Main genetic types and geological characteristics of iron-rich ore deposits in China. *Miner. Depos.* **2013**, *32*, 685–704. (In Chinese with English abstract)
38. Kimberley, M.M. Geochemical distinctions among environmental types of iron formations. *Chem. Geol.* **1979**, *25*, 185–212. [[CrossRef](#)]
39. Van Houten, F.B. Review of Cenozoic ooidal ironstones. *Sediment. Geol.* **1992**, *78*, 101–110. [[CrossRef](#)]
40. Bekker, A.; Planavsky, N.J.; Krapež, B.; Rasmussen, B.; Hofmann, A.; Slack, J.F.; Rouxel, O.J.; Konhauser, K.O. Iron formation: Their origins and implications for ancient seawater chemistry. In *Reference Module in Earth Systems and Environmental Sciences, Treatise on Geochemistry*; Holland, H., Turekian, K., Eds.; Elsevier: Amsterdam, The Netherlands, 2013; pp. 561–628.
41. Xiao, L.-L.; Liu, F.-L. Precambrian metamorphic history of the metamorphic complexes in the Trans-North China Orogen, North China Craton. *Acta Petrol. Sin.* **2015**, *31*, 3012–3044. (In Chinese with English abstract)
42. Tang, L.; Santosh, M.; Tsunogae, T.; Koizumi, T.; Hu, X.-K.; Teng, X.-M. Petrology, phase equilibria modelling and zircon U–Pb geochronology of Paleoproterozoic mafic granulites from the Fuping Complex, North China Craton. *J. Metamorph. Geol.* **2017**, *35*, 517–540. [[CrossRef](#)]
43. Tang, L.; Santosh, M. Neoarchean granite-greenstone belts and related ore mineralization in the North China Craton: An overview. *Geosci. Front.* **2018**, *9*, 751–768. [[CrossRef](#)]
44. Peng, P.; Zhai, M.-G.; Zhang, H.-F.; Guo, J.-H. Geochronological constraints on the Paleoproterozoic evolution of the North China Craton: SHRIMP zircon ages of different types of mafic dikes. *Int. Geol. Rev.* **2005**, *47*, 492–508. [[CrossRef](#)]
45. Zhang, J.; Tian, H.; Li, H.-K.; Su, W.-B.; Zhou, H.-Y.; Xiang, Z.-Q.; Geng, J.-Z.; Yang, L.-G. Age, geochemistry and zircon Hf isotope of the alkaline basaltic rocks in the middle section of the Yan-Liao aulacogen along the northern margin of the North China Craton: New evidence for the breakup of the Columbia Supercontinent. *Acta Petrol. Sin.* **2015**, *31*, 3129–3146. (In Chinese with English abstract)
46. Bureau of Geology and Mineral Resources of Hebei Province. In *Regional Geology of Hebei Province, Beijing Municipality and Tianjin Municipality*; Geological Publishing House: Beijing, China, 1992; pp. 1–741. (In Chinese)
47. Tang, D.-J.; Shi, X.-Y.; Liu, D.-B.; Lin, Y.-T.; Zhang, C.-H.; Song, G.-Y.; Wu, J.-J. Terminal Paleoproterozoic ooidal ironstone from North China: A sedimentary response to the initial breakup of Columbia Supercontinent. *Earth Sci.* **2015**, *40*, 290–304. (In Chinese with English abstract)
48. Zhao, D.-X. Microstructures of ferruginous oolite and their genetic characteristics in the Xuanlong iron deposit, Hebei Province. *Sci. Geol. Sin.* **1994**, *29*, 71–77. (In Chinese with English abstract)
49. Zhao, Y. The Geochemistry Character of the Xuanlong Iron Deposit in Chuanlinggou Formation and Its Sedimentary Environment Significance. Master's Thesis, China University of Geosciences, Beijing, China, 2016. (In Chinese with English abstract)
50. Hou, K.-J.; Li, Y.-H.; Tian, Y.-R. In situ U-Pb zircon dating using laser ablation-multi ion counting-ICP-MS. *Miner. Depos.* **2009**, *28*, 481–492. (In Chinese with English abstract)
51. Liu, Y.-S.; Gao, S.; Hu, Z.-C.; Gao, C.-G.; Zong, K.-Q.; Wang, D.-B. Continental and oceanic crust recycling-induced melt-peridotite interactions in the Trans-North China Orogen: U-Pb dating, Hf isotopes and trace elements in zircons from mantle xenoliths. *J. Petrol.* **2010**, *51*, 537–571. [[CrossRef](#)]
52. Jackson, S.E.; Pearson, N.J.; Griffin, W.L.; Belousova, E.A. The application of laser ablation-inductively coupled plasma-mass spectrometry to in situ U-Pb zircon geochronology. *Chem. Geol.* **2004**, *211*, 47–69. [[CrossRef](#)]
53. Ludwig, K.R. User's manual for Isoplot 3.0: A Geochronological Toolkit for Microsoft Excel. *Berkeley Geochronol. Cent. Spec. Publ.* **2003**, *4*, 1–71.

54. Sláma, J.; Kosler, J.; Condon, D.J.; Crowley, J.L.; Gerdes, A.; Hanchar, J.M.; Horstwood, M.S.A.; Morris, G.A.; Nasdala, L.; Norberg, N. Plesovice zircon—A new natural reference material for U-Pb and Hf isotopic microanalysis. *Chem. Geol.* **2008**, *249*, 1–35. [[CrossRef](#)]
55. Chu, N.-C.; Taylor, R.N.; Chavagnac, V.; Nesbitt, R.W.; Boella, R.M.; Milton, J.A.; German, C.R.; Bayon, G.; Burton, K. Hf isotope ratio analysis using multi-collector inductively coupled plasma mass spectrometry: An evaluation of isobaric interference corrections. *J. Anal. At. Spectrom.* **2002**, *17*, 1567–1574. [[CrossRef](#)]
56. Wu, F.-Y.; Yang, Y.-H.; Xie, L.-W.; Yang, J.-H.; Xu, P. Hf isotopic compositions of the standard zircons and baddeleyites used in U-Pb geochronology. *Chem. Geol.* **2006**, *234*, 105–126. [[CrossRef](#)]
57. Hou, K.-J.; Li, Y.-H.; Zou, T.-R.; Qu, X.-M.; Shi, Y.-R.; Xie, G.-Q. Laser ablation-MC-ICP-MS technique for Hf isotope microanalysis of zircon and its geological applications. *Acta Petrol. Sin.* **2007**, *23*, 2595–2604. (In Chinese with English abstract)
58. Morel, M.L.A.; Nebel, O.; Nebel-Jacobsen, Y.J.; Miller, J.S.; Vroon, P.Z. Hafnium isotope characterization of the GJ-1 zircon reference material by solution and laser-ablation MC-ICPMS. *Chem. Geol.* **2008**, *255*, 231–235. [[CrossRef](#)]
59. Blichert-Toft, J.; Albarede, F. The Lu-Hf isotope geochemistry of chondrites and the evolution of the mantle-crust system. *Earth Planet. Sci. Lett.* **1997**, *148*, 243–258. [[CrossRef](#)]
60. Griffin, W.L.; Wang, X.; Jackson, S.E.; Pearson, N.J.; O'Reilly, S.Y. Zircon geochemistry and magma mixing, SE China: In situ analysis of Hf isotopes, Tonglu and Pingtan igneous complexes. *Lithos* **2002**, *61*, 237–269. [[CrossRef](#)]
61. Soderlund, U.; Patchett, P.J.; Vervoort, J.D.; Isachsen, C.E. The  $^{176}\text{Lu}$  decay constant determined by Lu-Hf and U-Pb isotope systematics of Precambrian mafic intrusions. *Earth Planet. Sci. Lett.* **2004**, *219*, 311–324. [[CrossRef](#)]
62. Hoskin, P.W.O.; Schaltegger, U. The composition of zircon and igneous and metamorphic petrogenesis. *Rev. Mineral. Geochem.* **2003**, *53*, 27–62. [[CrossRef](#)]
63. Croft, F.; Hanchar, J.M.; Hoskin, P.W.; Kinny, P. Atlas of zircon textures. *Rev. Mineral. Geochem.* **2003**, *53*, 469–500. [[CrossRef](#)]
64. Belousova, E.A.; Griffin, W.L.; O'Reilly, S.Y.; Fisher, N.I. Igneous zircon: Trace element composition as an indicator of source rock type. *Contrib. Mineral. Petrol.* **2002**, *143*, 602–622. [[CrossRef](#)]
65. Koschek, G. Origin and significance of the SEM cathodoluminescence from zircon. *J. Microsc.* **1993**, *171*, 223–232. [[CrossRef](#)]
66. Gao, L.-Z.; Zhang, C.-H.; Liu, P.-J.; Ding, X.-Z.; Wang, Z.-Q.; Zhang, Y.-J. Recognition of Meso- and Neoproterozoic Stratigraphic Framework in North and South China. *Acta Geosci. Sin.* **2009**, *30*, 433–446. (In Chinese with English abstract)
67. Zhang, S.-H.; Zhao, Y.; Ye, H.; Hu, J.-M.; Wu, F. New constraints on ages of the Chuanlinggou and Tuanshanzi formations of the Changcheng System in the Yan-Liao area in the northern North China Craton. *Acta Petrol. Sin.* **2013**, *29*, 2481–2490. (In Chinese with English abstract)
68. Sun, H.-Y.; Gao, L.-Z.; Bao, C.; Chen, Y.-L.; Liu, D.-Y. SHRIMP zircon U-Pb of Mesoproterozoic Chuanlinggou formation from Kuancheng County in Hebei Province and its geological implication. *Acta Geol. Sin.* **2013**, *87*, 591–596. (In Chinese with English abstract)
69. He, Z.-J.; Niu, B.-G.; Zhang, X.-Y.; Zhao, L.; Liu, R.-Y. Discovery of the paleo-weathered mantle of the rapakivi granite covered by the Proterozoic Changzhougou Formation in the Miyun area, Beijing and their detrital zircon dating. *Geol. Bull. China* **2011**, *30*, 798–802. (In Chinese with English abstract)
70. Li, H.-K.; Su, W.-B.; Zhou, H.-Y.; Geng, J.-Z.; Xiang, Z.-Q.; Cui, Y.-R.; Liu, W.-C.; Lu, S.-N. The base age of the Changchengian System at the northern North China Craton should be younger than 1670 Ma: Constraints from zircon U-Pb LA-MC-ICPMS dating of a granite-porphyry dike in Miyun County, Beijing. *Earth Sci. Front.* **2011**, *18*, 108–120. (in Chinese with English abstract)
71. Li, H.-K.; Lu, S.-N.; Su, W.-B.; Xiang, Z.-Q.; Zhou, H.-Y.; Zhang, Y.-Q. Recent advances in the study of the Mesoproterozoic geochronology in the North China Craton. *J. Asian Earth Sci.* **2013**, *72*, 216–227. [[CrossRef](#)]
72. Liu, D.-Y.; Nutman, A.P.; Compston, W.; Wu, J.-S.; Shen, Q.-H. Remnants of 3800 Ma crust in the Chinese part of the Sino-Korean Craton. *Geology* **1992**, *20*, 339–342. [[CrossRef](#)]
73. Song, B.; Nutman, A.P.; Liu, D.Y.; Wu, J.-S. 3800 to 2500 Ma crust in the Anshan area of Liaoning Province, northeastern China. *Precambrian Res.* **1996**, *78*, 79–94. [[CrossRef](#)]
74. Wu, F.-Y.; Zhang, Y.-B.; Yang, J.-H.; Xie, L.-W.; Yang, Y.-H. Zircon U-Pb and Hf isotopic constraints on the Early Archean crustal evolution in Anshan of the North China Craton. *Precambrian Res.* **2008**, *167*, 339–362. [[CrossRef](#)]

75. Wan, Y.-S.; Liu, D.-T.; Song, B.; Wu, J.-S.; Yang, C.-H.; Zhang, Z.-Q.; Geng, Y.-S. Geochemical and Nd isotopic compositions of  $\geq 3.8$  Ga meta-quartz dioritic and trondhjemite rocks from the Anshan area and their geological significance. *J. Asian Earth Sci.* **2005**, *24*, 563–575. [[CrossRef](#)]
76. Wan, Y.-S.; Liu, D.-Y.; Dong, C.-Y.; Nutman, A.; Wilde, S.A.; Wang, W.; Xie, H.-Q.; Yin, X.-Y.; Zhou, H.-Y. The oldest rocks and zircons in China. *Acta Petrol. Sin.* **2009**, *25*, 1793–1807. (In Chinese with English abstract)
77. Tang, L.; Santosh, M. Neoarchean-Paleoproterozoic terrane assembly and Wilson cycle in the North China Craton: An overview from the central segment of the Trans North China Orogen. *Earth-Sci. Rev.* **2018**, *182*, 1–27. [[CrossRef](#)]
78. Zhai, M.-G.; Liu, W.-J. Palaeoproterozoic tectonic history of the North China Craton: A review. *Precambrian Res.* **2003**, *122*, 183–199. [[CrossRef](#)]
79. Lu, S.-N.; Yang, C.-L.; Li, H.-K.; Chen, Z.-H. North China continent and Columbia supercontinent. *Earth Sci. Front.* **2002**, *9*, 225–233. (In Chinese with English abstract)
80. Zhao, G.-C.; Wilde, S.A.; Cawood, P.A.; Sun, M. SHRIMP U–Pb zircon ages of the Fuping Complex: Implications for accretion and assembly of the North China Craton. *Am. J. Sci.* **2002**, *302*, 191–226. [[CrossRef](#)]
81. Rogers, J.J.W.; Santosh, M. Configuration of Columbia, a Mesoproterozoic supercontinent. *Gondwana Res.* **2002**, *5*, 5–22. [[CrossRef](#)]
82. Santosh, M.; Sajeev, K.; Li, J.-H. Extreme crustal metamorphism during Columbia supercontinent assembly: Evidence from North China Craton. *Gondwana Res.* **2006**, *10*, 256–266. [[CrossRef](#)]
83. Windley, B.F. *The Evolving Continents*, 3rd ed.; John Wiley and Sons: New York, NY, USA, 1995.
84. Yu, J.-H.; Fu, H.-Q.; Haapala, I.; Ramo, T.O.; Vaasjoki, M.; Mortensen, J.K. A 1.70 Ga anorogenic rapakivi granite suite in the northern part of North China Craton. *J. Geol. Miner. Res. North China* **1996**, *11*, 341–350.
85. Rämö, O.T.; Haapala, I.; Vaasjoki, M.; Yu, J.-H.; Fu, H.-Q. 1700 Ma Shachang complex, northeast China: Proterozoic rapakivi granite not associated with Paleoproterozoic orogenic crust. *Geology* **1995**, *23*, 815–818. [[CrossRef](#)]
86. Zhao, T.-P.; Chen, F.-K.; Zhai, M.-G.; Xia, B. Single zircon U–Pb ages and their geological significance of the Damiao anorthosite complex, Hebei Province, China. *Acta Petrol. Sin.* **2004**, *20*, 685–690. (In Chinese with English abstract)
87. Zhao, T.-P.; Zhou, M.-F.; Zhai, M.-G.; Xia, B. Paleoproterozoic rift-related volcanism of the Xiong'er group, North China Craton: Implications for the breakup of Columbia. *Int. Geol. Rev.* **2002**, *44*, 336–351. [[CrossRef](#)]
88. Peng, P.; Zhai, M.-G.; Zhang, H.-F.; Zhao, T.-P.; Ni, Z.-Y. Geochemistry and geological significance of the 1.8Ga mafic dyke swarms in the North China Craton: An Example from the juncture of Shanxi, Hebei and Inner Mongolia. *Acta Petrol. Sin.* **2004**, *20*, 439–456. (In Chinese with English abstract)
89. Peng, P.; Zhai, M.-G.; Guo, J.-H.; Kusky, T.; Zhao, T.-P. Nature of mantle source contributions and crystal differentiation in the petrogenesis of the 1.78 Ga mafic dykes in the central North China Craton. *Gondwana Res.* **2007**, *12*, 29–46. [[CrossRef](#)]
90. Lu, S.-N.; Yang, C.-L.; Li, H.-K.; Li, H.-M. A group of rifting events in the terminal Paleoproterozoic in the North China Craton. *Gondwana Res.* **2002**, *5*, 123–131.
91. Ren, K.-X.; Yan, G.-H.; Cai, J.-H.; Mu, B.-L.; Li, F.-T.; Wang, Y.-B.; Chu, Z.-Y. Geochronology and geological implication of the Pale-Mesoproterozoic alkaline-rich intrusions belt from the northern part in the North China Craton. *Acta Petrol. Sin.* **2006**, *22*, 377–386. (In Chinese with English abstract)
92. Yang, J.-H.; Wu, F.-Y.; Liu, X.-M.; Xie, L.-W. Zircon U–Pb ages and Hf isotopes and their geological significance of the Miyun rapakivi granites from Beijing, China. *Acta Petrol. Sin.* **2005**, *21*, 1633–1644. (In Chinese with English abstract)
93. Yang, D.-B.; Xu, W.-L.; Xu, Y.-G.; Wang, Q.-H.; Pei, F.-P.; Wang, F. U–Pb ages and Hf isotope data from detrital zircons in the Neoproterozoic sandstones of northern Jiangsu and southern Liaoning Provinces, China: Implications for the Late Precambrian evolution of the southeastern North China Craton. *Precambrian Res.* **2012**, *216–219*, 162–176. [[CrossRef](#)]
94. Liu, C.-H.; Liu, F.-L. The Mesoproterozoic rifting in the North China Craton: A case study for magmatism and sedimentation of the Zhaertai-Bayan Obo-Huade rift zone. *Acta Petrol. Sin.* **2015**, *31*, 3107–3128. (In Chinese with English abstract)
95. Diwu, C.-R.; Sun, Y.; Zhang, H.; Wang, Q.; Guo, A.-L.; Fan, L.G. Episodic tectonothermal events of the western North China Craton and North Qinling Orogenic Belt in central China: Constraints from detrital zircon U–Pb ages. *J. Asian Earth Sci.* **2012**, *47*, 107–122. [[CrossRef](#)]

96. Wu, C.-H.; Li, H.-M.; Zhong, C.-T.; Zuo, Y.-C. TIMS U-Pb single zircon ages for the orthogneisses and paragneisses of Fuping Complex. *Prog. Precambrian Res.* **2000**, *23*, 130–139.
97. Guo, J.-H.; Sun, M.; Zhai, M.-G. Sm–Nd and SHRIMP U–Pb zircon geochronology of high-pressure granulites in the Sangan area, North China Craton: Timing of Paleoproterozoic continental collision. *J. Asian Earth Sci.* **2005**, *24*, 529–542. [[CrossRef](#)]
98. Li, T.-S.; Zhai, M.-G.; Peng, P.; Chen, L.; Guo, J.-H. Ca. 2.5 billion year old coeval ultramafic-mafic and syenitic dykes in Eastern Hebei: Implications for cratonization of the North China Craton. *Precambrian Res.* **2010**, *180*, 143–155. [[CrossRef](#)]
99. Geng, Y.-S.; Liu, F.-L.; Yang, C.-H. Magmatic event at the end of the Archean in eastern Hebei Province and its geological implication. *Acta Geol. Sin.* **2006**, *80*, 819–833.
100. Hawkesworth, C.J.; Kemp, A.I.S. Using hafnium and oxygen isotopes in zircons to unravel the record of crustal evolution. *Chem. Geol.* **2006**, *226*, 144–162. [[CrossRef](#)]
101. Wu, F.-Y.; Li, X.-H.; Zheng, Y.-F.; Gao, S. Lu–Hf isotopic systematics and their applications in petrology. *Acta Petrol. Sin.* **2007**, *23*, 185–220. (In Chinese with English abstract)
102. Zheng, Y.-F.; Zhang, S.-B.; Zhao, Z.-F.; Wu, Y.-B.; Li, X.-H.; Li, Z.-X.; Wu, F.-Y. Contrasting zircon Hf and O isotopes in the two episodes of Neoproterozoic granitoids in South China: Implications for growth and reworking of continental crust. *Lithos* **2007**, *96*, 127–150. [[CrossRef](#)]
103. Iizuka, T.; Yamaguchi, T.; Itano, K.; Hibiya, Y.; Suzuki, K. What Hf isotopes in zircon tell us about crust–mantle evolution. *Lithos* **2017**, *274–275*, 304–327. [[CrossRef](#)]
104. Geng, Y.-S.; Du, L.-L.; Ren, L.-D. Growth and reworking of the early Precambrian continental crust in the North China Craton: Constraints from zircon Hf isotopes. *Gondwana Res.* **2012**, *21*, 517–529. [[CrossRef](#)]
105. Zhang, J.; Zhang, H.-F.; Lu, X.-X. Zircon U–Pb age and Lu–Hf isotope constraints on Precambrian evolution of continental crust in the Songshan area, the south-central North China Craton. *Precambrian Res.* **2013**, *226*, 1–20. [[CrossRef](#)]
106. Wan, Y.-S.; Liu, D.-Y.; Wang, S.-J.; Yang, E.-X.; Wang, W.; Dong, C.-Y.; Zhou, H.-Y.; Du, L.-L.; Yang, Y.-S.; Diwu, C.-R. ~2.7 Ga juvenile crust formation in the North China Craton (Taishan-Xintai area, western Shandong Province): Further evidence of an understated event from U–Pb dating and Hf isotopic composition of zircon. *Precambrian Res.* **2011**, *186*, 169–180. [[CrossRef](#)]
107. Ying, J.-F.; Zhou, X.-H.; Xu, B.-X.; Tang, Y.-J. Continental growth and secular evolution: Constraints from U–Pb ages and Hf isotope of detrital zircons in Proterozoic Jixian sedimentary section (1.8–0.8 Ga), North China Craton. *Precambrian Res.* **2011**, *189*, 229–238. [[CrossRef](#)]
108. Sun, J.-F.; Yang, J.-H.; Wu, F.-Y.; Wilde, S.A. Precambrian crustal evolution of the eastern North China Craton as revealed by U–Pb ages and Hf isotopes of detrital zircons from the Proterozoic Jing’eryu Formation. *Precambrian Res.* **2012**, *200–203*, 184–208. [[CrossRef](#)]
109. Liu, J.-H.; Liu, F.-L.; Ding, Z.-J.; Yang, H.; Liu, C.-H.; Liu, P.-H.; Xiao, L.-L.; Zhao, L.; Geng, J.-Z. U–Pb dating and Hf isotope study of detrital zircons from the Zhifu Group, Jiaobei Terrane, North China Craton: Provenance and implications for Precambrian crustal growth and recycling. *Precambrian Res.* **2013**, *235*, 230–250. [[CrossRef](#)]
110. Zhang, J.-X.; Gong, J.-H.; Yu, S.-Y.; Li, H.-K.; Hou, K.-J. Neoarchean–Paleoproterozoic multiple tectonothermal events in the western Alxa block, North China Craton and their geological implication: Evidence from zircon U–Pb ages and Hf isotopic composition. *Precambrian Res.* **2013**, *235*, 36–57. [[CrossRef](#)]
111. Zhang, H.-F.; Zhang, J.; Zhang, G.-W.; Santosh, M.; Yu, H.; Yang, Y.-H.; Wang, J.-L. Detrital zircon U–Pb, Lu–Hf, and O isotopes of the Wufoshan Group: Implications for episodic crustal growth and reworking of the southern North China craton. *Precambrian Res.* **2016**, *273*, 112–128. [[CrossRef](#)]
112. Wang, W.; Zhai, M.-G.; Li, T.S.; Santosh, M.; Zhao, L.; Wang, H.-Z. Archean–Paleoproterozoic crustal evolution in the eastern North China Craton: Zircon U–Th–Pb and Lu–Hf evidence from the Jiaobei terrane. *Precambrian Res.* **2014**, *241*, 146–160. [[CrossRef](#)]
113. Wu, F.-Y.; Zhao, G.-C.; Wilde, S.A.; Sun, D.-Y. Nd isotopic constraints on crustal formation in the North China Craton. *J. Asian Earth Sci.* **2005**, *24*, 523–545. [[CrossRef](#)]

